The Effect of Increasing Temperature on Greenhouse Gas Emissions by *Halophila stipulacea* in the Red Sea

Thesis by

Celina Burkholz

In Partial Fulfillment of the Requirements

For the Degree of

Master of Science

King Abdullah University of Science and Technology

Thuwal, Kingdom of Saudi Arabia

December, 2018

EXAMINATION COMMITTEE PAGE

The thesis of Celina Burkholz is approved by the examination committee

Committee Chairperson: Professor Carlos M. Duarte
Committee Members: Professor Xosé Anxelu G. Morán, Professor Daniele Daffonchio

ABSTRACT

The effect of increasing temperature on greenhouse gas emissions by *Halophila stipulacea* in the Red Sea

Celina Burkholz

Seagrass ecosystems are intense carbon sinks, but they can also emit greenhouse gases (GHG), such as carbon dioxide (CO_2) and methane (CH_4), to the atmosphere. Yet, GHG emissions by seagrasses are not considered when estimating global CH_4 production rates by natural sources, although these estimations will help predict future scenarios and potential changes in CH_4 emissions. In addition, the effect of warming on GHG emissions by seagrasses has not yet been reported. The present study aims to assess the CO_2 and CH_4 production rates by vegetated and adjacent bare sediment of a monospecific seagrass meadow (*Halophila stipulacea*) located in the central Red Sea. We measured CH_4 and CO_2 fluxes and their isotopic signatures by cavity ring-down spectroscopy on chambers containing vegetated and bare sediment. The fluxes were measured at temperatures from 25 °C (winter seawater temperature) to 37 °C to cover the natural thermal range and future seawater temperatures in the Red Sea. Additional parameters analyzed included changes in the sediment microbial community composition, sediment organic matter, organic carbon, nitrogen, and phosphorus concentration. We detected up to 100-fold higher CH_4 (up tp 571.65 µmol CH_4 m^{-2} d−1) and up to six-fold higher CO_2 (up to 13,930.18 µmol CO_2 m^{-2} d−1) fluxes in vegetated sediment compared to bare sediment, and an increase in CH_4 and CO_2 production with increasing temperature. In contrast, CH_4 and CO_2 production rates decreased in communities that were maintained at 25 °C, while communities that were exposed to prolonged darkness showed a decrease in CH_4 and an increase in CO_2 production rates. However, only minor changes were seen in the microbial community

composition with increasing temperatures. These results show that GHG emissions by seagrasses might be affected by natural temperature extremes and warming due to climate change in the Red Sea. The findings will have critical implications for the estimation of natural GHG sources, especially when predicting future changes in the global CH_4 budget.

ACKNOWLEDGEMENTS

I would like to thank my supervisor Professor Carlos M. Duarte for his guidance throughout the project, as well as the committee, Professor Xosé Anxelu G. Morán and Professor Daniele Daffonchio, for their time assessing this thesis and giving valuable feedback.

I am very grateful for the endless support of Dr. Neus Garcias Bonet; her guidance, patience and help throughout the entire process.

This research was made possible due to the help of many people involved. Thank you to Kathrine Rowe and the Coastal and Marine Resources Core Lab (CMOR) for their help during field work. CMOR also kindly provided support with the experimental set-up.

My appreciation goes out to Paloma Carrillo de Albornoz, Mongi Ennasri, Vijayalaxmi Dasari and Dr. Ruben Díaz Rúa for taking the time to teach me new methods, and for their help with sample processing. I would also like to thank Kiruthiga Gayathri Mariappan and Anny Cardenas for their support with data analysis.

TABLE OF CONTENTS

LIST OF ABBREVIATIONS

ANOVA	Analysis of Variance
C	Carbon
$CaCO_3$	Calcium Carbonate
CAP	Constrained Analysis of Principal Coordinates
CH_4	Methane
CMOR	Coastal and Marine Resources Core Lab
CO_2	Carbon Dioxide
CRDS	Cavity Ring-Down Spectrometer
DNA	Deoxyribonucleic Acid
DW	Dry Weight
GHG	Greenhouse Gases
GWP	Global Warming Potential
HCl	Hydrochloric Acid
HNO_3	Nitric Acid
LOI	Loss on Ignition
MDS	Multidimensional Scaling
N	Nitrogen
OTU	Operational Taxonomic Unit
P	Phosphorus
PCR	Polymerase Chain Reaction
PVC	Polyvinyl chloride

LIST OF SYMBOLS

β	Bunsen Solubility Coefficient
δ	Variation of isotopic ratios between an element and a standard

LIST OF FIGURES

LIST OF TABLES

1 Introduction

1.1 Climate change

The Earth's climate has always been changing due to natural causes. However, since 1950, there is a clear trend that the climate system is now influenced by human activity (Potts, 2018). Results of this activity are a rise in global temperature, increased seawater temperature, an increase in the number and intensity of severe weather events, reduced ice and snow cover, ocean acidification and accelerated sea level rise (Ledley et al., 1999; Potts, 2018). All these changes will have tremendous effects on terrestrial and marine organisms and ecosystems worldwide.

The global annual surface temperature for land and ocean combined has increased by 0.85 °C between 1880 to 2012 (IPCC, 2014). By the end of the 21^{st} century, the global mean surface temperature is predicted to increase by 0.3 - 1.7 °C, under a mitigation scenario (RCP 2.6), to 2.6 - 4.8 °C, under a business-as-usual scenario (RCP 8.5) compared to pre-industrial times (Collins et al., 2013) (Fig. 1).

Increasing temperatures can lead to a shift in the key species and result in altered ecosystem functions (Hoegh-Guldberg and Bruno, 2010). In coral reefs, rising temperatures result in corals expelling their symbionts, i.e. coral bleaching, which can ultimately end in the loss of biodiversity (Hoegh-Guldberg, 1999). If a reef cannot recover from such a disturbance, corals will be overgrown by algae resulting in a coral-algal phase shift (McManus and Polsenberg, 2004). This in turn will not only change the fish community but the entire food web structure. Other benthic ecosystems such as macrophyte communities will be affected as well (Duarte et al., 2018a). Increased temperatures can negatively affect seagrass ecosystems (Short and Neckles, 1999) as well as macroalgal forests (Piñeiro-Corbeira et al., 2018).

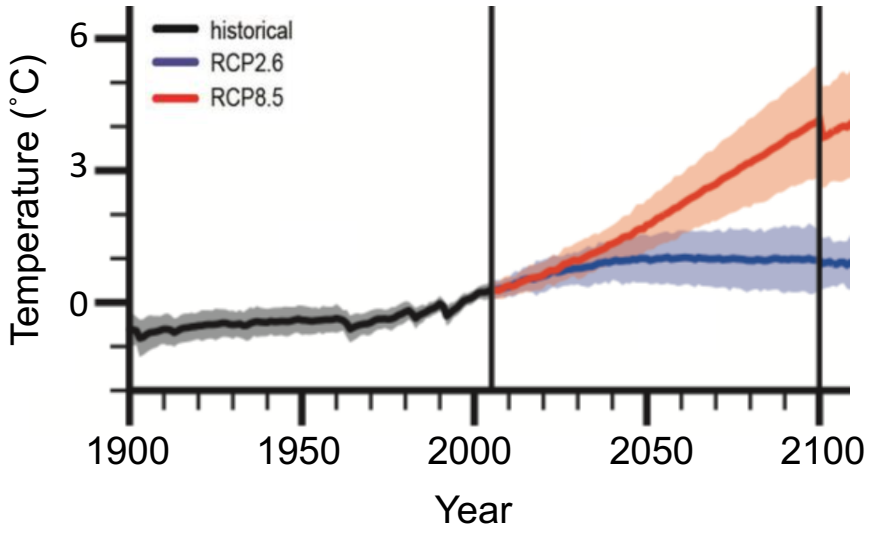

Figure 1: Global average surface temperature change from 1900 - 2100 (relative to 1986-2005). Projections show mean (solid lines) and the 5 to 95 % range (shading). Lines and shading represent historical simulations (grey), a mitigation scenario (RCP 2.6, purple) and a business-as-usual scenario (RCP 8.5, red). Adapted from IPCC (2014).

The capacity of the ocean to act as a carbon (C) sink will weaken due to climate change (Sarmiento and Le Quéré, 1996) and will contribute to an increase in atmospheric greenhouse gas concentrations (Joos et al., 1999). The effects of climate change can therefore have tremendous consequences for marine ecosystems, their functions, and for societies relying on them (Allison et al., 2009; Hoegh-Guldberg and Bruno, 2010).

1.2 Greenhouse gases and blue carbon

Climate change is driven by greenhouse gases (Ledley et al., 1999), which absorb infrared light in the atmosphere and thereby contribute to retain heat and affect the global climate. Only small changes in the concentration of these gases can have tremendous consequences for the average temperature on Earth. How strong and

effective a greenhouse gas is, can be determined by its Global Warming Potential (GWP), its atmospheric residence time and its concentration. The GWP of methane (CH_4), the second strongest greenhouse gas, is 28 times higher than carbon dioxide (CO_2), the strongest greenhouse gas, on a 100 year time scale, even though the atmospheric concentration of CO_2 is about 200 times higher than CH_4 (Myhre et al., 2013). The global mixing ratio of CH_4 increased from 722 $\pm$ 25 ppb in 1750 to 1803 $\pm$ 2 ppb in 2011, while the concentration of CO_2 increased from 278 to 391 $\pm$ 0.2 ppm (Myhre et al., 2013) (Fig. 2). The lifetime of CH_4 is estimated to be 12.4 years (Myhre et al., 2013), while the residence time of CO_2 can only be roughly estimated between 5 - 200 years (Albritton et al., 2001).

CH_4 can be emitted by either biogenic, thermogenic and pyrogenic sources, which include natural and anthropogenic sources (Kirschke et al., 2013). Terrestrial and aquatic sources emitting CH_4 include wetlands, dams, organic waste deposits, cattle and livestock, marine seeps, exploitation of coal and the incomplete combustion of fossil fuels amongst others (Kirschke et al., 2013). CO_2 can also be emitted by natural (i.a. ocean, animal and plant respiration) and anthropogenic (i.a. burning of fossil fuels, deforestation) sources. Le Quéré et al. (2009) found that fossil fuel emissions increased by 29 % between 2000 and 2008, while 43 % of CO_2 emissions between 1959 and 2008 were not sequestered in carbon sinks, but remained in the atmosphere instead. This increase has led to an imbalance of the carbon cycle and intensified the greenhouse effect. For both CO_2 and CH_4, the sources are characterized by different isotopic $\delta^{13}C$ signatures which allow to determine the source (Kirschke et al., 2013).

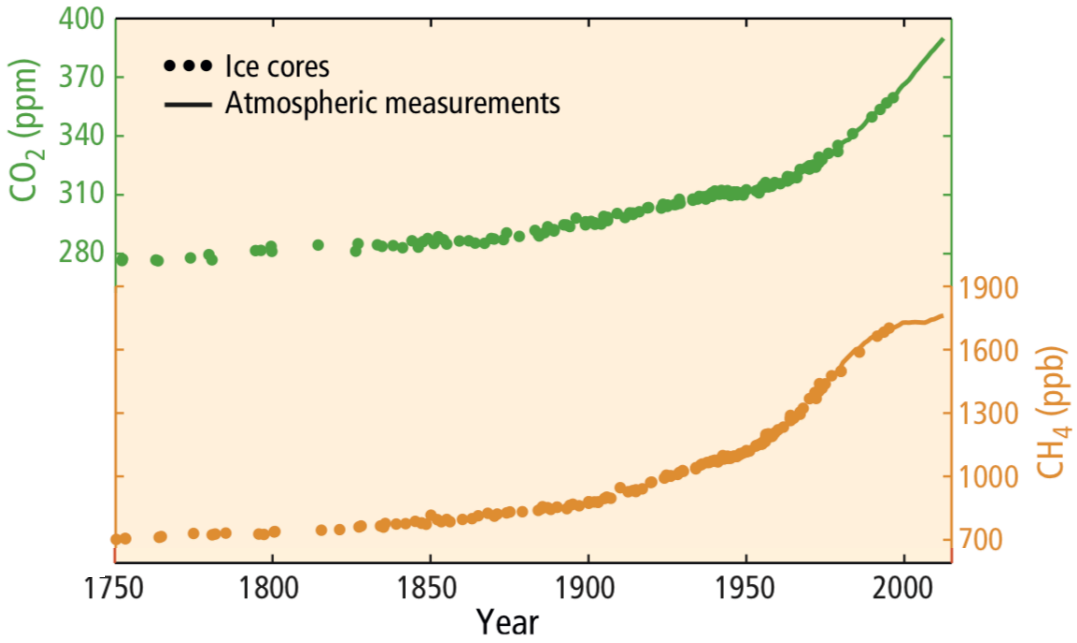

Figure 2: Globally averaged greenhouse gas (carbon dioxide (CO_2, green) and methane (CH_4, orange)) concentrations from ice cores (symbols) and atmospheric measurements (lines). Adapted from IPCC (2014).

The ocean is a main carbon sink balancing the emissions of natural sources as well as absorbing some of the anthropogenic carbon emissions through physical, chemical, and biological processes (Le Quéré et al., 2009; McLeod et al., 2011). 25 % of the CO_2 emitted by anthropogenic activity has been absorbed by the oceans (Potts, 2018). Blue carbon, the carbon sequestered by vegetated coastal ecosystems, is also an important factor in regulating greenhouse gas absorption (Duarte et al., 2005; McLeod et al., 2011). Blue carbon ecosystems, such as mangroves, salt marshes and seagrass meadows, accumulate organic C that would otherwise contribute, as CO_2 or CH_4, to the greenhouse effect (Duarte et al., 2005). Seagrasses are known to be autotrophic ecosystems, acting as carbon sinks (Duarte et al., 2010) supporting a global burial rate of 27.4 Tg C yr^{-1} (Duarte et al., 2005). They store carbon in their below- and above-ground biomass on a short term as well as in their sediment long-term (Duarte et al., 2005) up to millennia (Mateo et al., 1997). They account for 10 % of the carbon storage in ocean sediments even though they only cover 0.2 % of the

ocean surface (Duarte et al., 2005; Fourqurean et al., 2012a). However, disturbances can lead to the loss of biomass and the emissions of stored carbon turning blue carbon ecosystems into carbon sources (Macreadie et al., 2015; Lovelock et al., 2017; Arias-Ortiz et al., 2018) which will ultimately contribute to global GHG emissions intensifying the greenhouse effect.

1.3 Seagrass ecosystems

Seagrass ecosystems rank among the most productive (Duarte and Chiscano, 1999) and economically valuable ecosystems in the world (Costanza et al., 1997), and can be found worldwide except for Antarctica. Besides their important role as a blue carbon ecosystem, seagrass meadows offer other important ecosystem services such as removal of bacterial pathogens (Lamb et al., 2017), protection of archaeological heritage (Krause-Jensen et al., 2018), coastal stabilization, nurseries and removal of nutrients (Orth et al., 2006) (Fig. 3).

Seagrasses have also shown to be natural sources of CH_4 with average production rates ranging from 1.4 - 401.3 µmol CH_4 m^{-2} d^{-1} (Oremland, 1975; Barber and Carlson, 1993; Alongi et al., 2008; Deborde et al., 2010; Bahlmann et al., 2015; Garcias-Bonet and Duarte, 2017). Even though it was thought that CH_4 production rates by plants only play a minor role in the global budget (Kirschke et al., 2013), Garcias-Bonet and Duarte (2017) reported that seagrasses could contribute to global CH_4 emissions by releasing CH_4 at a rate of 0.09 - 2.7 Tg yr^{-1}. They estimated that CH_4 emissions by seagrasses might increase the contribution of marine global emissions to previously reported global estimates by about 30 % (Garcias-Bonet and Duarte, 2017). Lyimo et al. (2018) have also shown that stressors such as shading and grazing lead to an increase of CH_4 emissions by seagrass ecosystems by reducing their photosynthetic capacity.

In general, disturbances can lead to the loss of seagrass biomass and the emissions of blue carbon turning seagrass meadows into carbon sources (Pendleton et al., 2012). Pendleton et al. (2012) estimated that the conversion and degradation of seagrass ecosystems would lead to an emission of 0.05 - 0.33 Pg CO_2 yr^{-1} estimating a annual global loss of 0.4 - 2.6 %. This in turn will contribute to the global carbon emissions intensifying the greenhouse effect. Since the 1990s, the world has already lost an estimated 50 % of seagrass meadows globally (McLeod et al., 2011) and is losing seagrass ecosystems at an alarming rate of 7 % yr^{-1} (Waycott et al., 2009) due to eutrophication, dredging, increased turbidity and boating (Orth et al., 2006) (Fig. 3). Rising temperatures and heatwaves are additional stressors that can lead to the reduction and loss of the ecosystem services of seagrasses (Pedersen et al., 2011), a decrease in productivity (Marsh et al., 1986) and an increase in mortality rate (Marbà and Duarte, 2010; Collier and Waycott, 2014; Arias-Ortiz et al., 2018). Induced seagrass mortality results in the release of sequestered carbon (Marbà et al., 2015; Arias-Ortiz et al., 2018) as disturbed parts of seagrass meadows have shown to have a lower soil organic carbon stock compared to undisturbed patches (Macreadie et al., 2015). By releasing CO_2 and CH_4, the loss of seagrass meadows will contribute to the component of global greenhouse gas emissions characterized as "land-use change" (Pendleton et al., 2012; Arias-Ortiz et al., 2018).

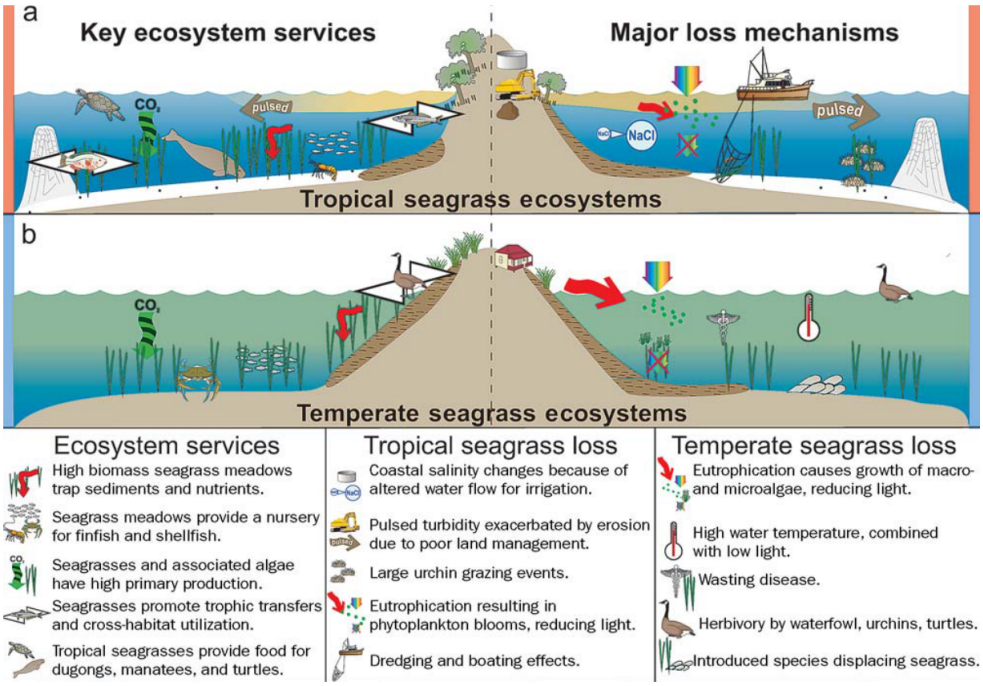

Figure 3: Ecosystem services and disturbances of tropical (a) and temperate (b) seagrass meadows. Adapted from Orth et al. (2006).

Sediment characteristics can also have an effect on the sequestration and emission of organic carbon. A higher nutrient load and high organic matter can promote an increase in CH_4 production (Sotomayor et al., 1994; Gonsalves et al., 2011). As organic matter is a vital factor in the emission of greenhouse gases, seagrass meadows provide favored conditions for the release of CO_2 and CH_4. Sediments in seagrass ecosystems support a 1.7-fold higher organic matter content than surrounding bare sediments, not only due to the slow turn-over of biomass but also due to their ability to trap particles (Duarte et al., 2013). In addition, these factors also lead to increased nitrogen and phosphorus contents in seagrass sediments (Fourqurean et al., 2012b). Estimating the nutrient contents can be used to define the nutrient availability for seagrasses (Gerloff and Krombholz, 1966). A higher nutrient availability, due to eutrophication, can lead to a change in species composition leaning towards fast-growing species (Fourqurean et al., 1995) or ultimately to seagrass mortality (Duarte, 1995), and also affect seagrass remineralization in the sediments (e.g. Enríquez et al. (1993)).

1.4 Microbial community composition

The fitness of a plant is not only affected by the plant itself but also by the microbial community composition, which together form the plant holobiont (Vandenkoornhuyse et al., 2015). The microbiota can affect the growth and survival of a plant as it is influenced by available nutrients and defense mechanisms to environmental stressors (Vandenkoornhuyse et al., 2015). In seagrasses, different microbial communities can be found in the phyllosphere, the endosphere and the rhizosphere (Ugarelli et al., 2017) (Fig. 4). Each compartment can be occupied by different communities as each part is characterized by different functions (Ugarelli et al., 2017). The microbial community composition in *H. stipulacea* has been shown to vary not only between compartments but also between sites (Meija et al., 2016). In other organisms such as corals, microbial communities are known to shift during coral bleaching induced by elevated temperature (Bourne et al., 2008). Stressors generally increase alpha and beta diversity as corals seem to be less resilient to microbes that are usually not part of their healthy microbiome (McDevitt-Irwin et al., 2017). In seagrasses, Hassenrück et al. (2015) have shown that the bacterial community on leaves of *E. acoroides* shifts under elevated pCO_2, while Macreadie et al. (2015) showed that disturbed patches in seagrass meadows have a higher abundance of aerobic heterotrophs compared to undisturbed areas. However, these results can vary with location, as Robador et al. (2009) showed that sulfate-reducing bacterial abundance declined in Arctic sediments under increasing temperature while this trend was not confirmed in temperate sediments. This could imply that this bacterial community composition is already adapted to seasonal temperature changes and therefore more resilient to elevated temperatures (Robador et al., 2009).

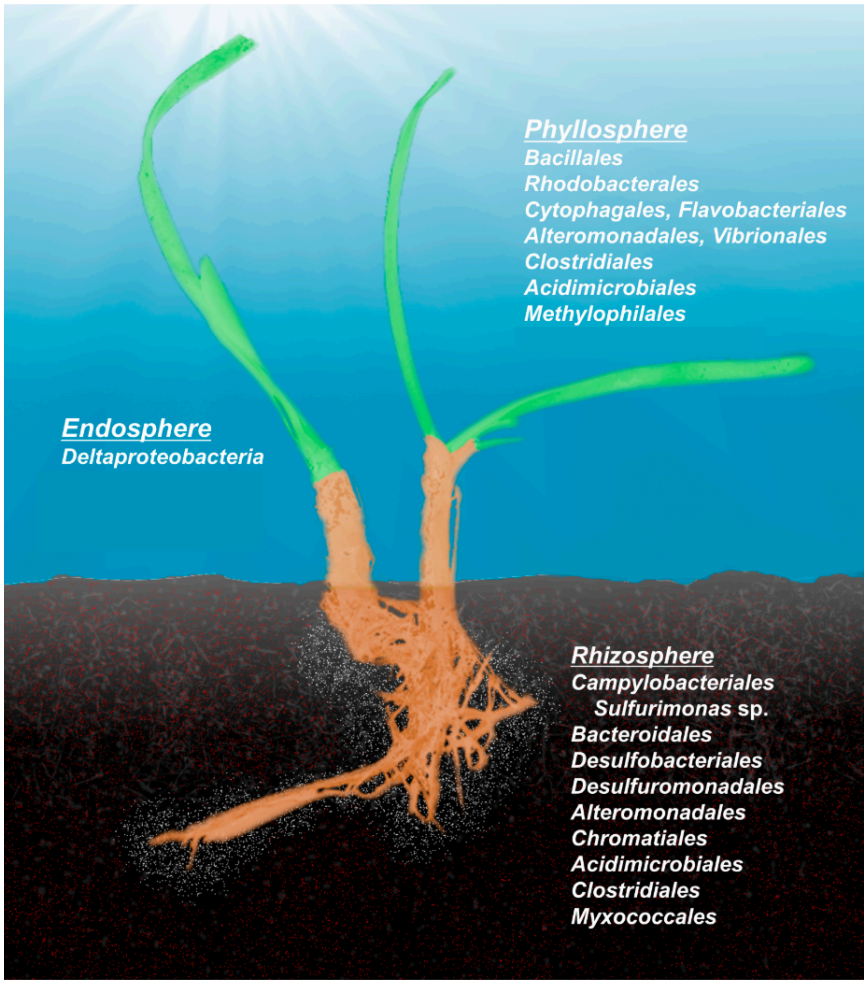

Figure 4: The most abundant bacterial groups in the different compartments. Adapted from Ugarelli et al. (2017).

Microbial communities also play an important role in the global carbon cycle. When organic matter is degraded in anaerobic conditions, the first step is hydrolysis which eventually results in CO_2 production. The final step, methanogenesis, is the production of CH_4 by anaerobic microbes, methanogens, that belong to the domain of archaea. The generated CH_4 can either be emitted to the atmosphere, or it can be used to support aerobic or anaerobic methane oxidation (Liu and Whitman, 2008).

1.5 Objectives of this study

Reports on greenhouse gas production rates by seagrass ecosystems are limited (Oremland, 1975; Barber and Carlson, 1993; Alongi et al., 2008; Deborde et al., 2010; Bahlmann et al., 2015; Garcias-Bonet and Duarte, 2017; Lyimo et al., 2018), and to date no reports have been published on how increasing seawater temperatures might affect these production rates. Additionally, it is currently unknown how the microbial community in seagrass sediments might shift under increasing seawater temperatures and what the consequences for their greenhouse gas production rates might be.

The Red Sea is a semi-enclosed sea basin that is warming at higher rates than other seas. It is characterized by high sea surface temperatures reaching up to 36 °C (Belkin, 2009; Chaidez et al., 2017) implying that seagrass ecosystems might already experience thermal stress. In addition to extreme temperatures, the Red Sea is also characterized by low nutrient concentrations. These factors have led to seagrasses in the Red Sea having lower carbon stocks compared to global values, yet these ecosystems are still an important carbon sink with a carbon stock of 3.4 ± 0.3 kg C_{org} m^{-2} (Serrano et al., 2018). The Red Sea therefore provides a unique study site that allows us to predict how seagrass meadows worldwide might change under rising seawater temperatures due to climate change.

The tropical seagrass species *Halophila stipulacea* (Forsskål) Ascherson (Fig. 5) is native to the Indian Ocean and one of the most common species in the Red Sea (El Shaffai, 2016). It seems to be highly adaptive to various environments, as it can now be found as an exotic species in the Mediterranean (Lipkin, 1975) and the Caribbean Sea (Ruiz and Ballantine, 2004), indicating its high resilience to changing conditions (Por, 1971), and was therefore the chosen study object.

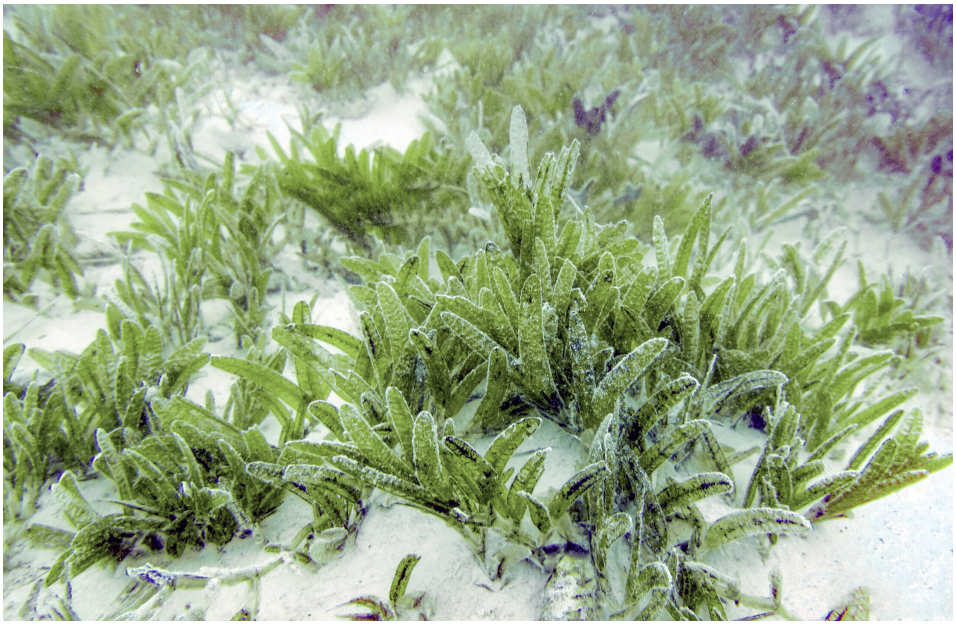

Figure 5: *Halophila stipulacea* in the Red Sea. Photo taken by C. Burkholz.

The aim of this study was to estimate the effects of increasing seawater temperature on greenhouse gas production rates by seagrass ecosystems. Additionally, prolonged darkness was chosen to test whether a different disturbance would lead to similar effects. Differences in the sediment composition were also analyzed to test for a potential relationship between the composition and the production rates.

1. The sediment composition of different meadows within an enclosed lagoon in the central Red Sea was characterized analyzing the organic carbon, nitrogen (N) and phosphorus (P) content, organic matter and carbonate content.

2. CO_2 and CH_4 production rates as well as their isotopic signatures were measured to evaluate the following:

   (a) Differences between different *H. stipulacea* meadows.

   (b) Differences between vegetated and adjacent bare sediment.

   (c) The effect of increasing seawater temperature in one *H. stipulacea* meadow.

   (d) The effect of prolonged darkness in one *H. stipulacea* meadow.

3. The effect of increasing temperature on the microbial community composition in seagrass sediments was experimentally examined.

2 Material and methods

2.1 Sample collection

Samples were collected at Al Kharar, a lagoon on the Saudi coast of the central Red Sea. Four *H. stipulacea* meadows (S1, S2, S3 and S4, Fig. 6) were chosen to to represent a range of organic matter content in the sediment, with two of those (S2 and S4), representing the lowest and highest organic matter content in the lagoon, selected to evaluate greenhouse gas production rates. One vegetated core in each meadow (two in S2) were collected and transferred to the laboratory. Above-ground biomass and the first 10 cm of sediment were collected and placed at 60 °C in a drying oven.

A dense *H. stipulacea* meadow in the middle of the lagoon (S4) was then chosen as the main study site to experimentally assess the role of temperature and darkness in greenhouse gas fluxes. The seagrass and sediment community was sampled using translucent cylindrical PVC cores (26 cm length and 9.5 cm in diameter). The sharpened edge of the core was carefully pushed approx. 10 cm into the sediment with a rubber hammer so that the structure of leaves, roots and sediment stayed intact. A rubber stopper was then placed on top, before the core was carefully pulled out of the sediment without disturbing the structure and another rubber stopper was placed on the bottom of the core.

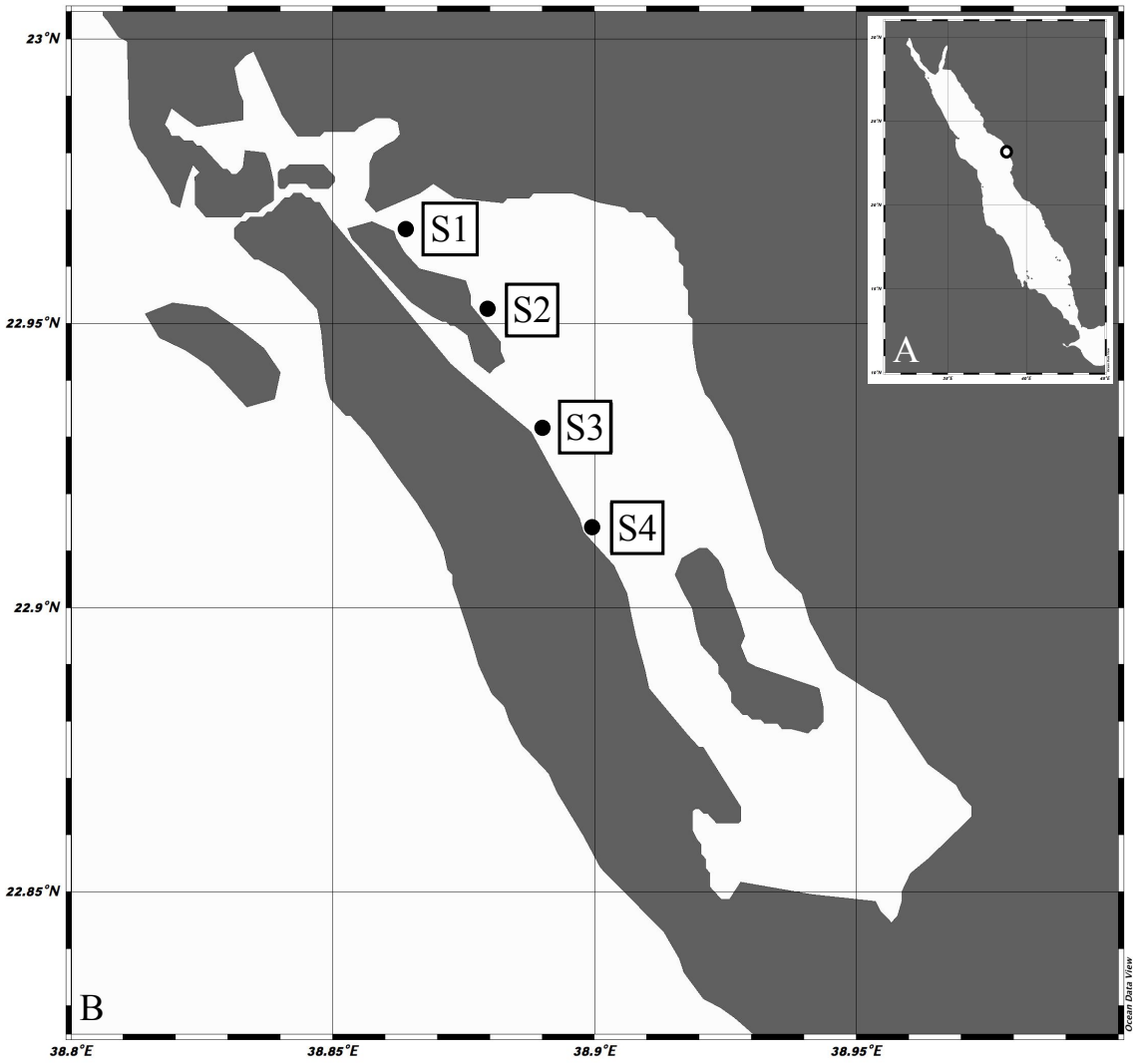

Figure 6: Locations of the study sites in the Red Sea (A) and a closer view of the different sites within the Al Kharar lagoon (B). Maps were modified from Ocean Data View Version 5.1.0 (Schlitzer, 2016).

2.2 Plant and sediment characterization

The sediment composition as well as nutrient analyses on plant parts and sediments were conducted to characterize different *H. stipulacea* meadows.

2.2.1 Sediment composition

Once the cores were opened, the first 10 cm of the sediment were collected and dried at 60 °C to a constant dry weight. Sediment was then ground for further analyses.

A 50 ml tube was filled with sediment from the first 10 cm and the contents dried at 60 °C to a constant dry weight and weighed to determine the sediment bulk density (g sediment cm^{-3}).

Organic matter content was analyzed by loss on ignition (LOI). Approx. 5 g of dried sediment were placed in pre-weighed crucibles. The crucibles were then placed in a muffler furnace and burned at 450 °C for 5 hours. Samples were weighed again and the organic matter content was calculated as

$$\%OM = \frac{\text{pre-ignition weight (g)} - \text{post-ignition weight (g)}}{\text{pre-ignition weight (g)}} \cdot 100 \qquad (1)$$

The carbonate content was estimated using a Pressure Gauge Calcimeter. Different concentrations of $CaCO_3$ were used to produce a calibration curve (0.2 g, 0.4 g, 0.6 g, 0.8 g, 1 g). Approx. 1 g of sample was placed in the calcimeter and the recipient was filled with 10 % hydrochloric acid (HCl). Once the recipient was carefully placed inside the calcimeter, the lid was closed and the calcimeter was agitated. The pressure was recorded every minute until maximum pressure was reached.

The mass of $CaCO_3$ in the sample (g) was then calculated as follows:

$$m_{CaCO_3} = \frac{p - b}{a \cdot w} \qquad (2)$$

where p is the pressure recorded (ppm), b is the slope and a the intercept derived from the calibration curve, and w is the exact weight of each sediment sample (g).

The percentage of $CaCO_3$ in the sample (% DW) was then calculated using Eq.

3:

$$\%_{CaCO_3} = \frac{m_{CaCO_3}}{w \cdot 100} \tag{3}$$

2.2.2 Plant and sediment nutrient analyses

Dried sediment and plant samples were digested using USEPA method 3052 and analyzed with nitric acid (HNO_3) and HCl using USEPA method 200.7. The phosphorus content (% DW) was analyzed using inductively coupled plasma optical emission spectroscropy (ICP-OES) on an Agilent 5110 ICP-OES (Agilent Technologies, Santa Clara, CA, USA). The C and N concentration of both plants and sediments was analyzed after acidification with HCl, using Flash 2000 Organic Elemental Analyzer (CHNS/O-2, Thermo Fisher Scientific, Waltham, MA, USA).

The isotopic signature of δ^{13}C in sediment organic matter was analyzed, using cavity ring-down spectroscropy (CRDS G2201-I, Picarro Inc., Santa Clara, CA, USA), from the δ^{13}C of CO_2 released by a combustion module (Costech Analytical Technologies Inc., CA, USA) delivering the CO_2 resulting from combusting the sediment organic matter to the CRDS instrument.

2.3 Experimental assessment of greenhouse gas fluxes

Greenhouse gas fluxes were assessed to test for differences in production rates by different *H. stipulacea* communities. The effect of warming on CH_4 and CO_2 production rates was analyzed as well as the changes in the microbial community composition. In addition, the effect of light vs. dark conditions on greenhouse gas fluxes were determined in order to assess the role of community photosynthesis in affecting the fluxes.

2.3.1 Methane and carbon dioxide fluxes in different *H. stipulacea* communities

Three cores each from vegetated and adjacent (distance about 5 m) bare sediments were collected from sites S2 and S4 and transferred to incubation chambers set at 25 °C and a 12 hours light (up to 70 µmol photons m^{-2} s^{-1}) : 12 hours dark (12 h L : 12 h D) cycle to measure the greenhouse gas (CO_2 and CH_4) fluxes supported by these communities.

Before measuring fluxes, the water inside the cores was replaced by fresh seawater from the aquaria leaving a headspace of approx. 5 - 6 cm, and the cores were closed again with stoppers containing gas-tight valves. The cores were left for one hour to allow for equilibration between the water and the headspace phase. We then sampled 10 mL of air from each core using a syringe, and injected the gases in a cavity ring-down spectrometer (CRDS; Picarro Inc., Santa Clara, CA, USA) through a small sample isotopic module extension (SSIM A0314, Picarro Inc., Santa Clara, CA, USA), which provided both the partial pressure and the isotopic carbon composition of the CO_2 and CH_4 in the sample.

Samples were taken at the start (T_0), after 12 hours of light (T_1) and after 12 hours of dark (T_2). Before and after each sampling, two standards were measured (A: 750 ppm CO_2, 9.7 ppm CH_4, B: 250.5 ppm CO_2, 3.25 ppm CH_4). The cores were then transferred back to the aquaria.

2.3.2 Effect of warming on methane and carbon dioxide fluxes

We collected 18 vegetated and 18 bare sediment cores (eight for flux measurements, ten for microbial community composition, respectively) to evaluate the response of greenhouse production rates to warming. The cores were then transferred to the Coastal and Marine Resources Core Lab (CMOR) and nine vegetated and nine bare cores were placed in each two aquaria with flow-through of seawater set at *in situ*

temperature (25 °C) and a 12 h L (up to 200 µmol photons m^{-2} s^{-1}) : 12 h D cycle.

One aquarium was maintained at 25 °C over the entire duration of the experiment to serve as a control for temperature-independent variability in fluxes. The temperature in the second aquarium was increased at a rate of 1 °C day^{-1}. CH_4 and CO_2 fluxes were measured at every 2 °C from 25 - 37 °C, with parallel measurements conducted on the cores maintained at 25 °C. After a one day acclimation period at each new temperature, the cores were closed with the stoppers and transferred to incubators (Percival chambers) set at the target seawater temperature for CO_2 and CH_4 flux measurements as described above. The cores were then returned to the aquaria.

An additional core kept at each of the constant temperature and warming sets was sampled every four days (i.e. at 4 °C temperature intervals in the warming treatment) to analyze sediment composition and microbial community composition. The cores used for fluxes estimates were then opened after the final measurement (i.e. 20 days since collection) to estimate the plant biomass, analyze the sediment composition and the microbial community composition at the end of the experiment.

2.3.3 Effect of darkness on methane and carbon dioxide fluxes

Six vegetated and six bare sediment cores were collected from site S4 and kept at a constant 25 °C with a 24 hours dark cycle. Only during the measurements in the incubators, the cores were exposed to a 12 h L : 12 h D cycle, so the fluxes could be compared with those measured in cores permanently maintained under the 12 h L : 12 h D photoperiod. CO_2 and CH_4 fluxes were measured after the first day of acclimation and then kept in the aquaria until signs of seagrass mortality started to become apparent, which occurred after one week in the dark. CO_2 and CH_4 fluxes were measured at alternate days. At the end of the experiment (21 days since collection), the cores were opened and sampled to assess plant biomass, sediment

composition and microbial community composition.

2.3.4 Methane and carbon dioxide measurements

The concentration of CO_2 in the seawater after equilibrium was calculated based on the concentration of CO_2 in the headspace (ppm) measured by CRDS according to Wilson et al. (2012) and Sea et al. (2018):

$$[CO_2]_w = 10^{-6}\beta m_a p_{dry} \tag{4}$$

where β is the Bunsen solubility coefficient of CO_2 (mol ml^{-1} atm^{-1}), m_a is the CO_2 concentration measured in the headspace (ppm), and p_{dry} is the atmospheric pressure of dry air (atm). The Bunsen solubility coefficient of CO_2 was calculated as follows:

$$\beta = H^{cp} \cdot (RT) \tag{5}$$

The R package marelac (Soetaert et al., 2010) was used to calculate the Henry consant H^{cp} (mol ml^{-1} atm^{-1}). R is the ideal gas constant (0.082057459 atm L mol^{-1} K^{-1}) and T is the standard temperature (273.15 K). The atmospheric pressure of dry air (p_{dry}) was calculated as follows:

$$p_{dry} = p_{wet}(1 - \%H_2O) \tag{6}$$

where p_{wet} is the atmospheric pressure of wet air. The Boyle's law was applied as gas was collected several times from the same core.

The concentration of dissolved CO_2 in seawater before equilibrium was then calculated using Eq. 7:

$$[CO_2]_{aq} = \frac{[CO_2]_w V_w + 10^{-6} m_a V_a}{V_w} \tag{7}$$

where V_w is the volume of seawater (mL) and V_a is the volume of the headspace

(mL).

The units were then converted to nM:

$$[CO_2]_{aq} = \frac{10^9 \cdot p_{dry}[CO_2]_{aq}}{RT} \tag{8}$$

The daily CO_2 fluxes were calculated from the difference between T_0 and T_2 taking into account the core surface area (µmol m^{-2} d^{-1}), and the light and dark fluxes were calculated from the change between CO_2 concentration after 12 hours of light and 12 hours of dark treatment, also transformed to an aerial basis (µmol m^{-2} h^{-1}).

The same calculations were used to estimate the daily and hourly CH_4 fluxes with the exception of the Bunsen solubility coefficient. The Bunsen solubility coefficient was calculated as a function of the seawater temperature and its salinity following Wiesenburg and Guinasso (1979).

Keeling plots were used to estimate the isotopic signature of CH_4 and CO_2 produced during the incubations, following Garcias-Bonet and Duarte (2017). $\delta^{13}C$ of CH_4 and CO_2 produced in the sediment was extracted from the intercept of the linear regression between the inverse of the gas concentration (ppm^{-1}) and the isotopic signature measured from the samples in the CDRS instrument.

2.4 Microbial composition analysis

Sediment (0 - 10 cm) samples were stored at -80 °C before extraction. Samples were defrosted and mixed before 0.25 - 0.5 g of sediment were transferred to PowerBead tubes. DNA extraction was conducted following the protocols of PowerSoil DNA Isolation Kit (MO BIO Laboratories Inc., Carlsbad, CA, USA) and SurePrep Soil DNA Isolation Kit (Fisher BioReagents, Thermo Fisher Scientific, Fair Lawn, NJ, USA). Samples were then quantified by QuBit (Quant-IT hsDNA High Sensitivity Assay

Kit; Invitrogen, Carlsbad, CA, USA). The V3 and V4 region of bacterial 16S rRNA gene was amplified using the primers 16S rRNA Amplicon PCR Forward Primer = 5' TCGTCGGCAGCGTCAGATGTGTATAAGAGACAGCCTACGGGNGGCWGCAG and 16S rRNA Amplicon PCR Reverse Primer = 5' GTCTCGTGGGCTCGGAGAT-GTGTATAAGAGACAGGACTACHVGGGTATCTAATCC, and the V4 region of archaeal 16S rRNA gene was amplified using the primers U519F (5'-CAG YMG CCR CGG KAA HAC C-3') and 806R (5'-GGA CTA CNN GGG TAT CTA AT-3'). For each sample, duplicate PCRs were run with a final volume of 40 µl using a primer concentration of 10 µM. The PCR conditions for bacterial 16S rRNA genes were as follows: One initial polymerase activation and denaturation cycle at 95 °C for 15 min, 30 cycles each at 95 °C for 30 s, 55 °C for 30 s, 72 °C for 30 s, followed by final elongation step at 72 °C for 5 min. The PCR conditions for archaeal 16S rRNA genes were as follows: One initial polymerase activation and denaturation cycle at 95 °C for 15 min, 27 cycles each at 94 °C for 15 s, 53 °C for 45 s, 68 °C for 45 s, followed by a final elongation step at 68 °C for 5 min. Successful amplification was visualized via 1 % agorose gel electrophoresis. For each sample, the duplicate PCR was pooled and cleaned with Agencourt AMPure XP magnetic bead system (Beckman Coulter, Brea, CA, USA). Following the manufacturer's protocol, the cleaned PCR products underwent an indexing PCR to add Nextera XT indexing and sequencing adapters (Illumina, San Diego, CA, USA). The Index PCR conditions were as follows: One cycle at 95 °C for 15 min, 8 cycles each at 95 °C for 30 s, 55 °C for 30 s, 72 °C for 30 s, followed by a final step at 72 °C for 5 min. Successful amplification was visualized via 2 % agorose gel electrophoresis and another cleaning step with Agencourt AMPure XP magnetic bead system (Beckman Coulter, Brea, CA, USA) followed. The cleaned products were then quantified by QuBit (Quant-IT hsDNA High Sensitivity Assay Kit; Invitrogen, Carlsbad, CA, USA) and Glomax Multi+ Detection plate reader (Promega, Madison, WI, USA), and pooled in equimolar ratios. The pooled product

was then checked on the BioAnalyzer (Agilent Technologies, Santa Clara, CA, USA) for presence of primer dimers. The sample was sequenced at 6 pM with 10% phiX on the Illumina MiSeq, $2 * 300$ bp paired-end version 3 chemistry according to the manufacturer's specifications.

Sequenced data set comprised 12,369,606 sequence reads distributed in 96 samples. Reads were trimmed to remove low quality bps using Trimmomatic 0.36 (Bolger et al., 2014). Trimmed reads were then error corrected using SPAdes 3.10.1 (Nurk et al., 2013). Error corrected reads were then merged using PEAR 0.9.10 (Zhang et al., 2014) using -u 0 -q 30 -p 0.0001 -n 0 -m 0 -v 50 for bacterial samples and -u 0 -q 30 -p 0.0001 -n 0 -m 0 -v 20 for archaeal samples. Merged reads were then analyzed using the software Mothur 1.39.5 (Schloss et al., 2009) by following the MiSeq SOP protocol. Sequences were assembled into 6,279,054 contigs for archaea and 5,048,002 for bacteria, and contigs with ambiguous bases, long homopolymers (>8) and insufficient length were removed. The sequences were then aligned against the SILVA database (release 132; Quast et al. (2013)) and pre-clustered with allowed difference of 2 bps. Chimeric sequences were removed (1,284,956 for archaea; 951,010 for bacteria) using VSEARCH 2.3.4 (Rogne et al., 2016) and sequences assigned to chloroplasts, mitochondria, archaea, eukaryotes, and other unwanted sequences from bacterial samples (36,235) and sequences assigned to chloroplasts, mitochondria, bacteria, eukaryotes, and other unknown sequences from archaeal samples (33,779) were excluded. Only sequences that were classified as bacteria for bacterial samples and archaea for archaeal samples (silva.nr_v132.tax; bootstrap = 80) were considered for further analyses. Sequences were then clustered into Operational Taxonomic Units (OTUs) using a 97% similarity cutoff.

2.5 Data analysis

The data was analyzed for normality using the Shapiro-Wilk test. Differences in nutrients between different plant parts, vegetated and bare sediment and sites were tested using t-test, one-way ANOVA, Mann-Whitney and Kruskal-Wallis test. To assess differences in greenhouse gas production rates between different *H. stipulacea* communities, differences in CH_4 and CO_2 production rates were analyzed between sites and between vegetated and bare sediment by using Mann Whitney and t-test. The effect of warming on greenhouse gas production rates was tested by using Kruskal-Wallis test and Dunn's multiple comparison test to assess differences between bare and vegetated sediments of the communities experiencing warming and the communities maintained at 25 °C. Trends in the flux between the communities experiencing warming and the ones maintained at 25 °C, as well as in the isotopic signature of δ^{13}C-CH_4 and δ^{13}C-CO_2 over time were analyzed by linear regression. When assessing the effect of darkness on greenhouse gas fluxes, the trend of the CH_4 and CO_2 production rates and their isotopic signatures were analyzed by linear regression. The statistical analyses were conducted in PRISM 5 (GraphPad Software, La Jolla, CA, USA) and JMP Pro 13.1.0 (SAS Institute Inc., Cary, NC, USA).

The microbial community composition was analyzed using the R software 1.1.442 (RCoreTeam, 2017) together with the package *Phyloseq* (McMurdie and Holmes, 2013). The differences in the archaeal and the bacterial community composition between the vegetated and bare sediment in the communities experiencing increasing temperatures and the ones that were maintained at 25 °C were analyzed on the phyla and family level. These analyses were conducted for OTU counts with an abundance > 2 %. The OTU counts were also visualized in Venn diagrams showing the number of OTU counts in common between vegetated sediment on day two and vegetated sediment of the increasing group on day 20. The alpha-diversity was assessed and

significant differences in the means between day two and say 20 were analyzed using t-test, when normally distributed, and Mann-Whitney when the data was not normally distributed. Differences between treatments and days were visualized with multidimensional scaling (MDS) and constrained analysis of principal coordinates (CAP), and Adonis permanova was used to test for significant differences between vegetated and bare sediment and the different communities maintained at 25 °C and exposed to warming from 25 - 37 °C.

3 Results

3.1 Seagrass and sediment composition

Nitrogen, carbon and phosphorus concentrations in seagrass leaves were relatively low, but nitrogen and carbon concentrations were about ten times greater than concentrations in the sediments (Fig. 7). Seagrass sampled in site S2 had both the highest nitrogen and carbon concentrations in the leaves, but the lowest phosphorus concentrations. The rhizomes tended to have lower carbon and nutrient concentration than the leaves (Fig. 8A, C and E), except for carbon in S4. In the sediment, the carbon and phosphorus concentrations were significantly different among sites (Kruskal-Wallis, $p < 0.05$, respectively), with the highest carbon and the lowest nitrogen concentrations found in the sediment of S4. There were no consistent differences in carbon and nutrient concentration in bare and vegetated sediments (Fig. 8B, D and F).

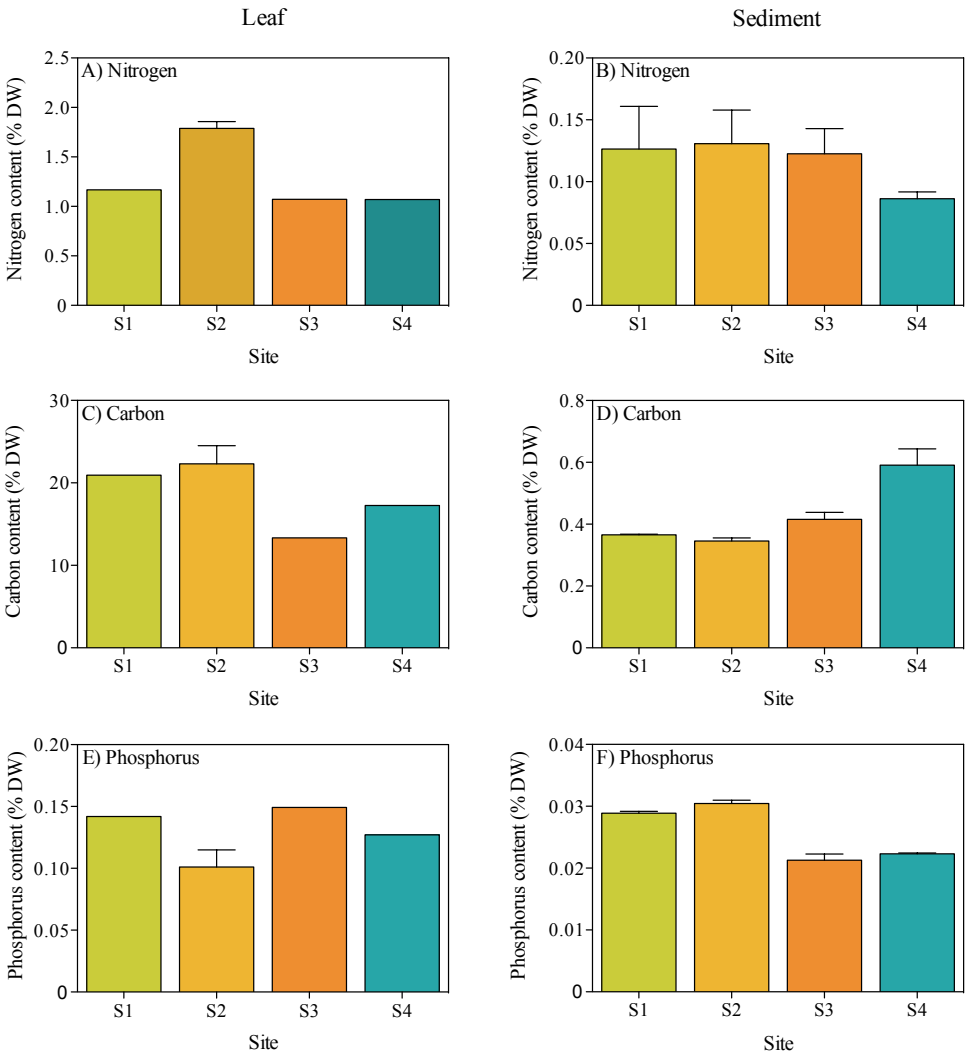

Figure 7: Mean + SE nutrient concentration in leaf (left) and sediment (right) per site. Nitrogen (A and B), carbon (C and D) and phosphorus (E and F) for sites S1, S2, S3 and S4.

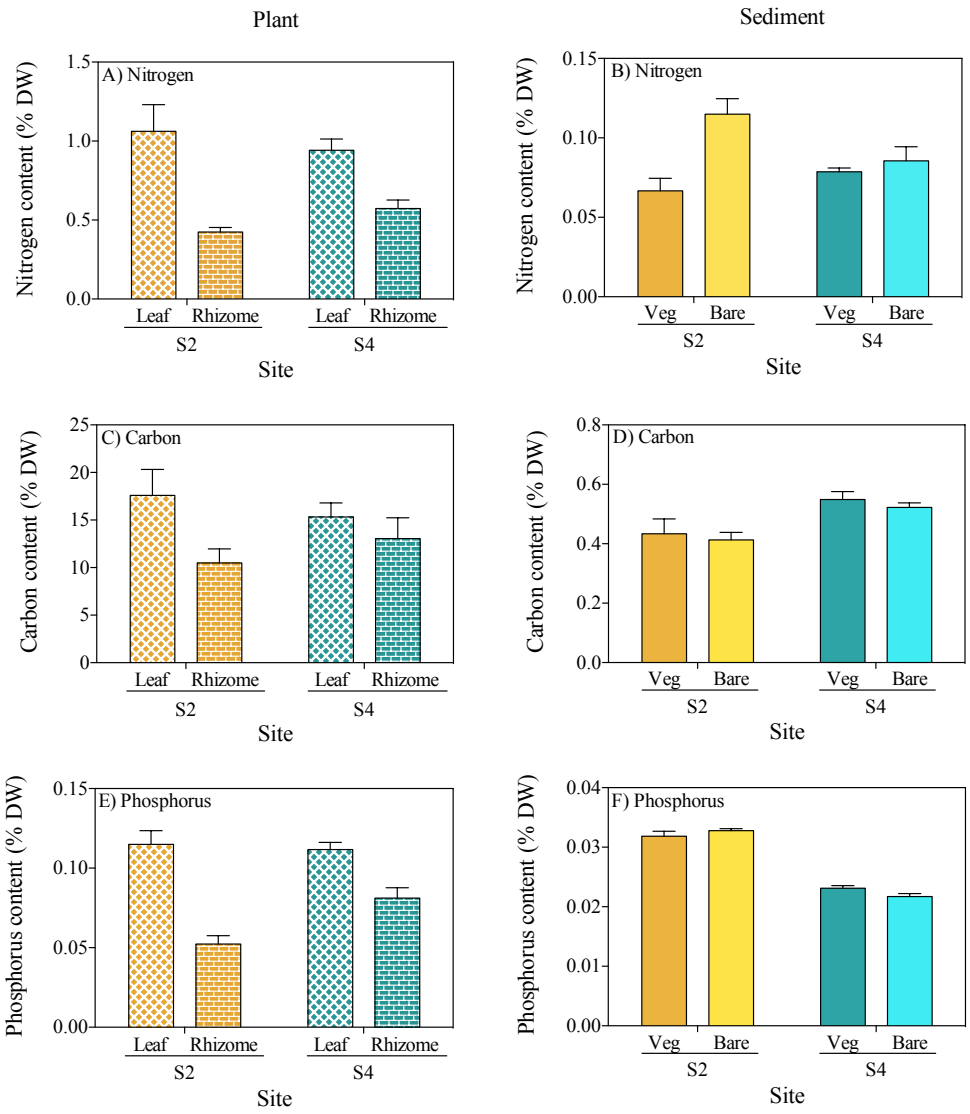

Figure 8: Mean + SE nutrient concentration in plant (left) and sediment (right) per site. Nitrogen (A and B), carbon (C and D) and phosphorus (E and F) for sites S2 and S4.

The sediments had high, but variable, carbonate concentrations, which differed among sites (ANOVA, $p < 0.05$) ranging from 82.41 % DW (at S4) to 92.49 $\pm$ 0.5 % DW (at S2) (Fig. 9A), while the organic matter content was highest in S4 (3.21 $\pm$ 0.06 % DW), but not significantly so (Kruskal-Wallis, $p > 0.05$; Fig. 9B). Sediment bulk density was similar in both S2 and S4 sites, ranging from 1.1 $\pm$ 0.07 to 1.28 $\pm$ 0.03 g cm^{-3}, but vegetated sediments in S2 showed significantly lower bulk density

compared to bare sediments (t-test, $p < 0.05$; Fig. 10). The isotopic signature of sediment organic carbon was around -16 ‰ across sites in both bare and vegetated sediments (Fig. 10).

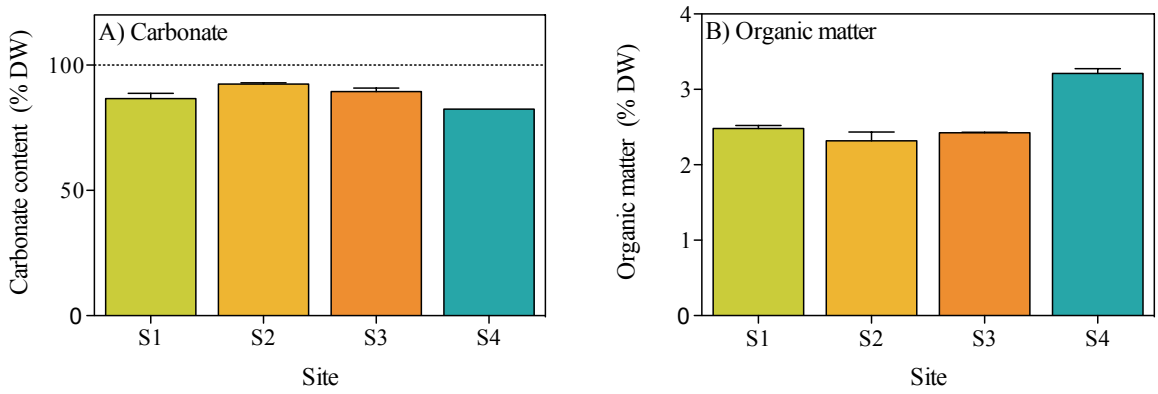

Figure 9: Mean + SE carbonate content (A) and organic matter content (B) at the sites S1, S2, S3 and S4.

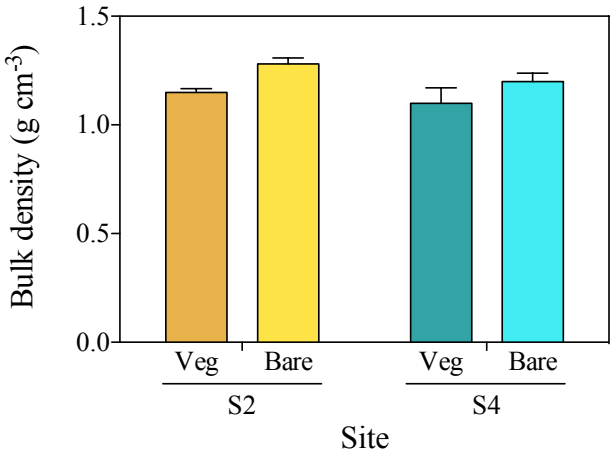

Figure 10: Mean + SE bulk density in vegetated and bare sediment per site S2 and S4.

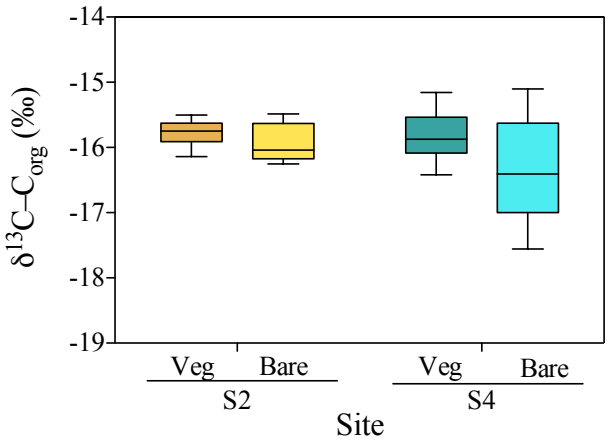

Figure 11: The isotopic signature of δ^{13}C for organic carbon in the vegetated and bare sediment of site S2 and S4. Whiskers indicate 5 and 95 %.

The nutrient concentrations in seagrass leaves and sediments showed fluctuations over time, regardless of whether temperature was held constant or increased (Fig. 12) and in bare and vegetated sediment (Fig. 13). There was no clear trend seen over the experimental time period.

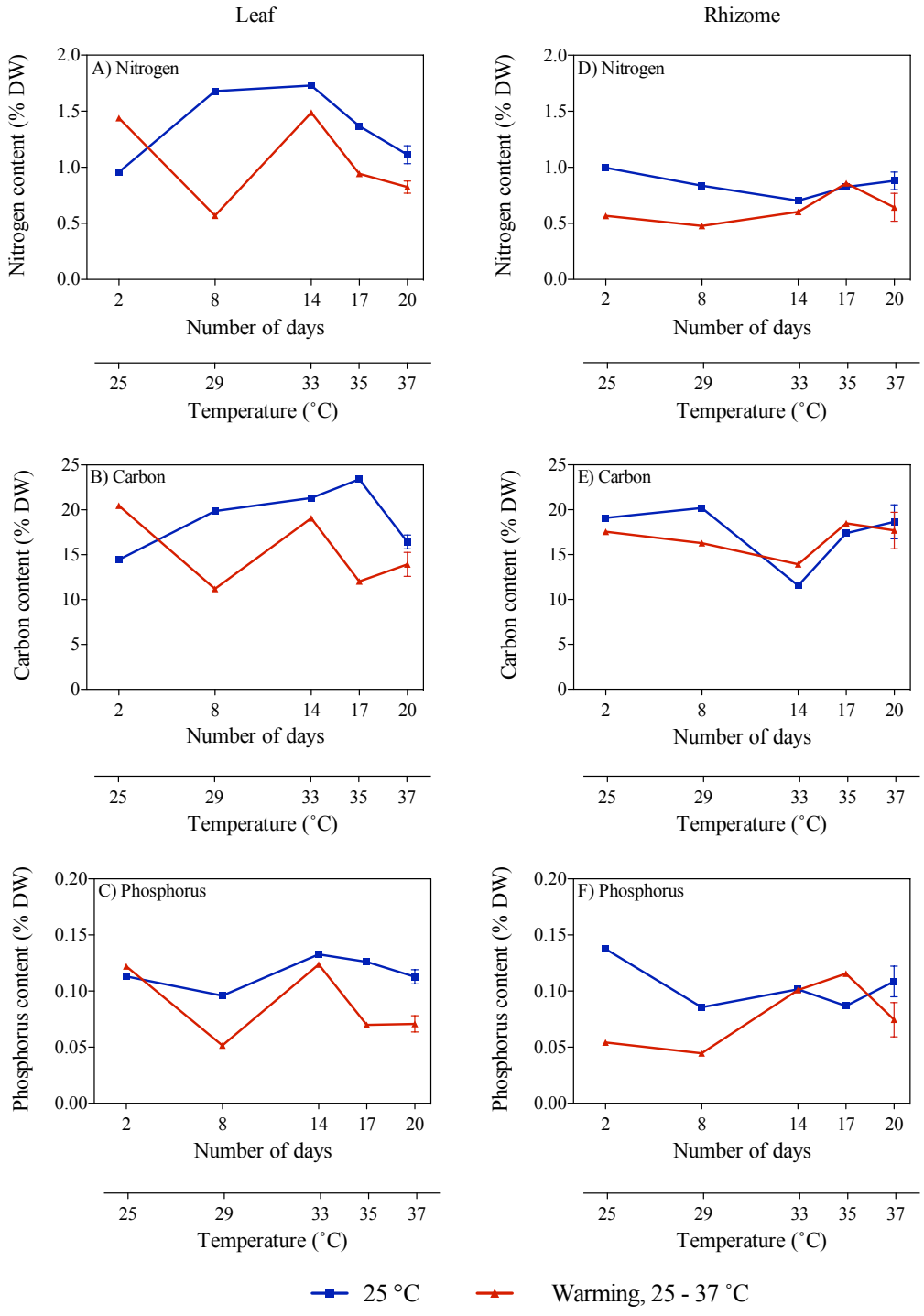

Figure 12: Mean ± SE nutrient concentration in leaf (left) and rhizome (right). Nitrogen (A and D), carbon (B and E) and phosphorus (C and F) content were measured in communities where temperature was maintained at 25 °C (blue) and those exposed to warming from 25 - 37 °C (red) over the experimental period (number of days since sample collection). The second x-axis indicates the temperature increase for the community experiencing warming.

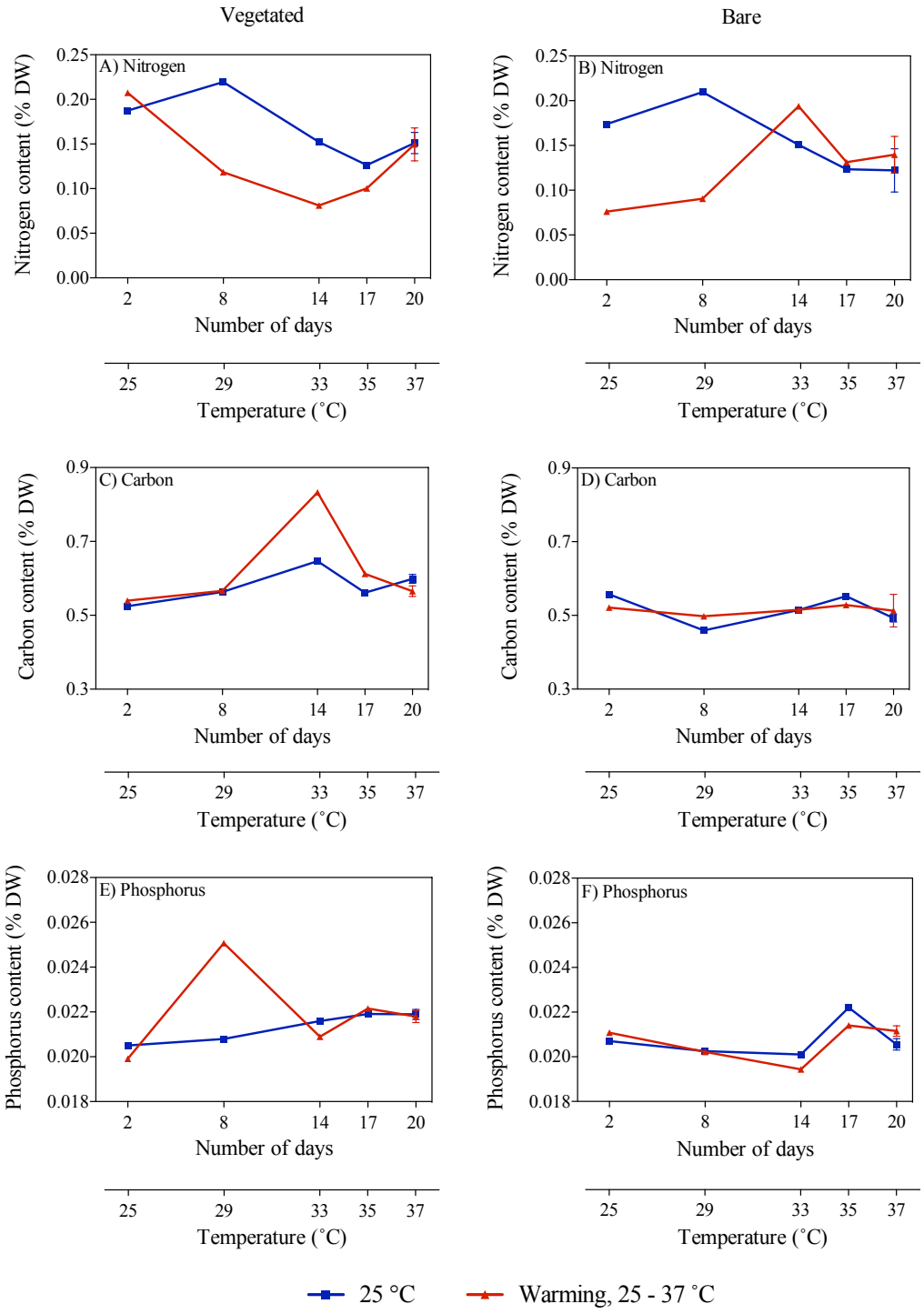

Figure 13: Mean + SE nutrient concentration in vegetated (left) and bare (right) sediment. Nitrogen (A and B), carbon (C and D) and phosphorus (E and F) content were measured communities where temperature was maintained at 25 °C (blue) and those exposed to warming from 25 - 37 °C (red) over the experimental period (number of days since sample collection). The second x-axis indicates the temperature increase for the community experiencing warming.

3.2 Methane and carbon dioxide fluxes

At both sites, S2 and S4, the daily net CH_4 production rate was 10- to 100-fold higher in vegetated compared to adjacent bare sediments (Mann-Whitney, $p < 0.05$; Fig. 14A). The daily CO_2 production rate was up to six-fold higher in vegetated compared to bare sediments, and tended to be generally higher in S4 compared to S2, where bare sediments showed net CO_2 uptake (Mann Whitney, $p < 0.05$; Fig. 14B).

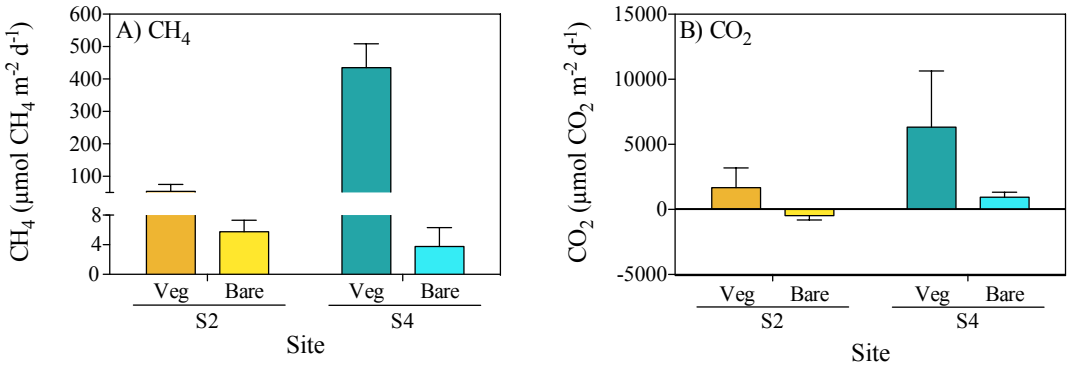

Figure 14: Mean + SE CH_4 (A) and CO_2 (B) production rates in the vegetated and bare sediment at site S2 and S4.

Net CH_4 production rates declined over time when the sediments were maintained at 25 °C ($R^2 = 0.43$, $p < 0.001$; Table 1; Fig. 15A). A similar trend was observed in the bare sediment with net CH_4 production rate declining over time when the sediments were maintained at 25 °C ($R^2 = 0.24$, $p < 0.001$; Fig. 15B). However, neither vegetated nor bare sediments showed significant differences between the communities maintained at 25 °C and the communities experiencing warming from 25 - 37 °C (Dunn's, $p > 0.05$, respectively). The flux, the difference between the communities experiencing warming and the ones maintained at 25 °C, showed a significant increase in the CH_4 production rates in the vegetated sediment ($R^2 = 0.69$, $p < 0.05$) but not in the bare sediment ($R^2 = 0.4$, $p > 0.05$; Fig. 16A).

Table 1: Mean ± SE CH_4 production rates measured in bare and vegetated communities maintained at 25 °C and in bare and vegetated communities exposed to warming from 25 - 37 °C. Days indicate the time since sample collection and temperature refers to the the communities exposed to warming.

	CH_4 production rate (µmol CH_4 m^{-2} d^{-1})				
	25 ˚C			25 - 37 ˚C	
Days	Bare	Vegetated	Temperature (˚C)	Bare	Vegetated
2	7.95 ± 4.56	59.67 ± 15.82	25	4.82 ± 4.14	54.1 ± 23.21
5	6.4 ± 2.09	82.2 ± 16.41	27	13.14 ± 5.92	57.33 ± 18.78
8	3.52 ± 1.75	49.01 ± 8.42	29	3.69 ± 1.51	48.79 ± 20.37
11	1.84 ± 0.76	41.21 ± 8.99	31	4.81 ± 1.72	47.94 ± 19.85
14	1.57 ± 0.35	26.69 ± 3.46	33	4.78 ± 1.69	19.65 ± 4.96
17	2.76 ± 1.21	28.43 ± 4.0	35	3.73 ± 0.93	68.65 ± 39.48
20	0.73 ± 0.22	18.45 ± 7.35	37	27.18 ± 19.62	88.11 ± 15.19

The net CO_2 production rate in the vegetated sediment increased greatly with warming ($R^2 = 0.38$, $p < 0.001$, Table 2), while it decreased over time from showing net CO_2 production to net CO_2 uptake when the community was maintained at 25 °C ($R^2 = 0.3$, $p < 0.01$; Dunn's, $p < 0.001$; Fig. 15C). Similar responses were observed in the bare sediments, where the net CO_2 production rate increased ($R^2 = 0.54$, $p < 0.0001$), while the community shifted from supporting net CO_2 production to a net CO_2 uptake when the community was maintained at 25 °C ($R^2 = 0.001$, $p > 0.05$; Fig. 15D). The flux of the CO_2 production rate increased significantly in both the vegetated and the bare sediment ($R^2 = 0.74$, $p < 0.05$ and $R^2 = 0.91$, $p < 0.001$, respectively, Fig. 16B).

An outlier in the vegetated sediment at 33 °C, day 14, was taken out of the data analysis. The net CH_4 production rate in this core was 699.81 CH_4 m^{-2} d^{-1} with a net CO_2 production of 55,169.49 CO_2 m^{-2} d^{-1} (Fig. 15A and B).

Table 2: Mean ± SE CO_2 production rates measured in bare and vegetated communities maintained at 25 °C and in bare and vegetated communities exposed to warming from 25 - 37 °C. Days indicate the time since sample collection and temperature refers to the the communities exposed to warming.

	CO_2 production rate (μmol CO_2 m^{-2} d^{-1})				
	25 ˚C			25 - 37 ˚C	
Days	Bare	Vegetated	Temperature (˚C)	Bare	Vegetated
2	175.72 ± 307.19	527.18 ± 605.17	25	73.76 ± 391.54	747.62 ± 590.24
5	-331.73 ± 44.79	-229.02 ± 498.39	27	184.16 ± 206.54	1798.24 ± 1762.62
8	-250.91 ± 129.42	-233.58 ± 393.44	29	315.07 ± 213.32	1024.33 ± 477.27
11	-382.96 ± 164.46	-820.06 ± 175.14	31	734.41 ± 372.15	1341.18 ± 278.32
14	-5.91 ± 114.24	-871.44 ± 281.91	33	1426.84 ± 255.33	1341.88 ± 405.25
17	89.49 ± 212.86	-804.09 ± 179.12	35	1298.08 ± 183.1	6058.69 ± 3141.78
20	-130.98 ± 214.6	-941.7 ± 208.15	37	1718.8 ± 402.69	10422.18 ± 2570.12

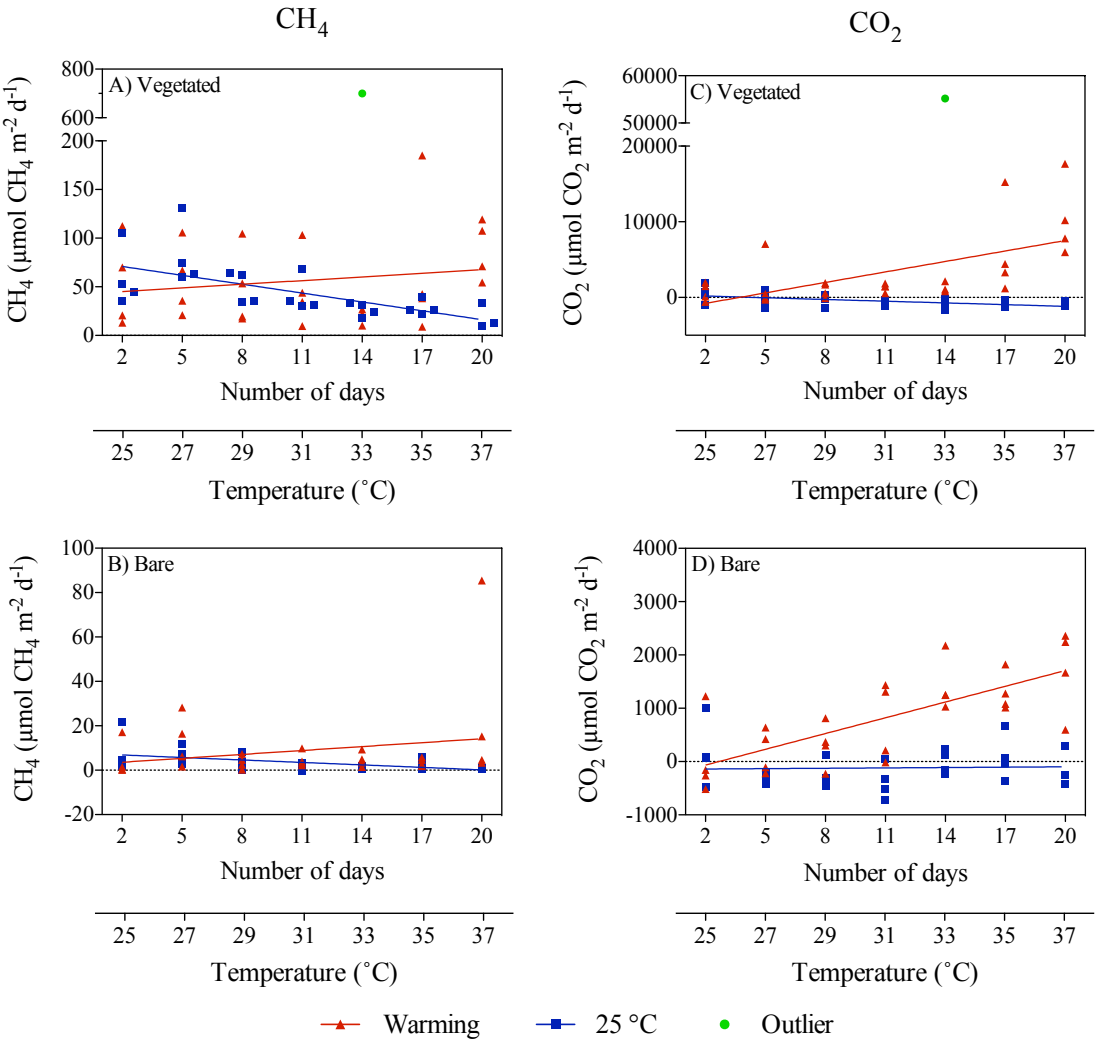

Figure 15: CH_4 (left) and CO_2 (right) production rates in vegetated (A and C) and bare (B and D) sediment. Symbols indicate each replicate of the community experiencing warming from 25 - 37 °C (red) and the community maintained at 25 °C (blue) over the experimental period (number of days since sample collection), as well as one outlier (green) at 33 °C. The second x-axis indicates the temperature increase for the community experiencing warming.

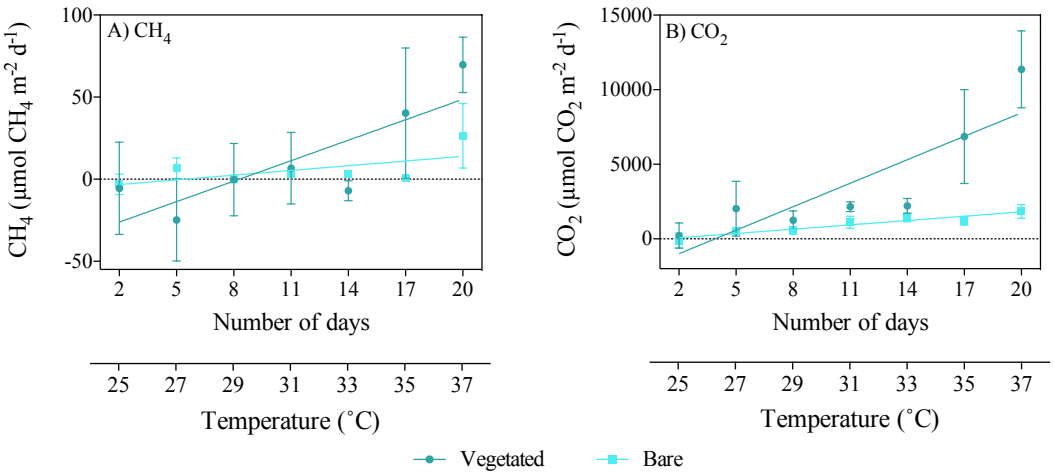

Figure 16: Mean ± SE CH_4 (A) and the CO_2 (B) fluxes in the vegetated (dark blue) and bare (light blue) sediment over the experimental period (number of days since sample collection). The second x-axis indicates the temperature increase for the community experiencing warming from 25 - 37 °C.

When vegetated sediments were kept in the dark, CH_4 production rates decreased five-fold significantly over time ($R^2 = 0.99$, $p < 0.0001$; Fig. 17A). The net CH_4 production rates did not differ significantly between vegetated cores maintained in the 12 h L : 12 h D photoperiod or in the dark (Mann Whitney, $p > 0.05$), as the same trend of decreasing CH_4 production rates was seen when the communities were maintained at 25 °C at a 12 h L : 12 h D photoperiod (Fig. 18A). In the bare sediment, CH_4 production rates were slightly decreasing, both when kept in the dark and in a 12 h L : 12 h D photoperiod, with prodcution rates with somewhat higher when kept in the dark. Significant differences were only seen on day 14 and day 20 (Mann Whitney, $p < 0.05$, respectively; Fig. 18B).

The vegetated sediment shifted over time from showing net CO_2 uptake to showing net CO_2 production when maintained in the dark ($R^2 = 0.7$, $p < 0.05$; Fig. 17B). In contrast, when vegetated sediment was maintained at 25 °C at a 12 h L : 12 h D photoperiod, a shift in the net CO_2 production rate was seen from net production to net uptake (Mann Whitney, $p < 0.05$; Fig. 18C). There was a similar fluctuation

seen in the bare sediment with no significant differences between communities at a 12 h L : 12 h D photoperiod and in the dark (Mann Whitney, $p > 0.05$; Fig. 18D).

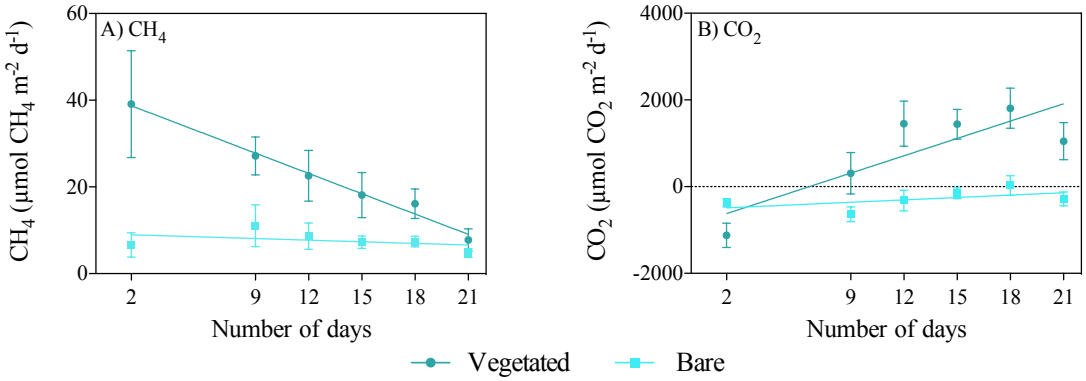

Figure 17: Mean ± SE CH_4 (A) and CO_2 (B) production rates in the vegetated (dark blue) and the bare (light blue) sediment in communities kept at 25 °C in darkness.

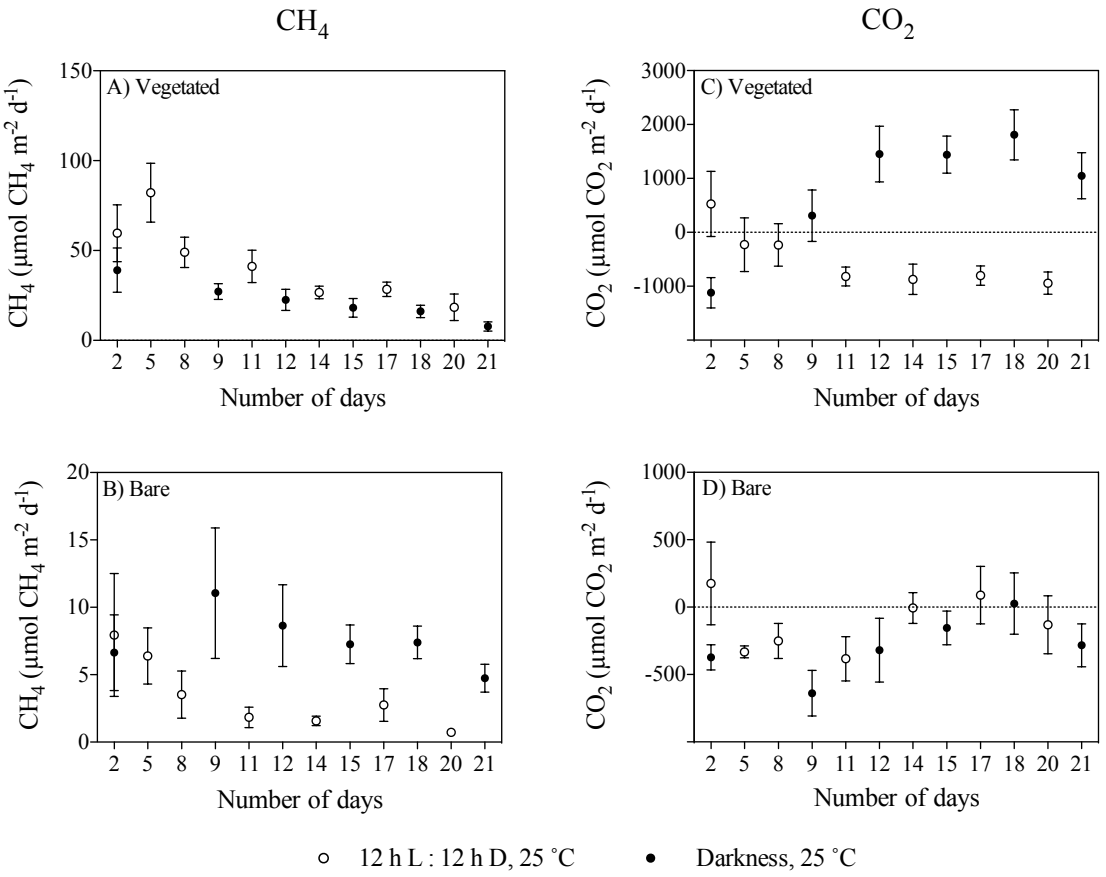

Figure 18: Mean ± SE CH_4 (left) and CO_2 (right) production rates in the vegetated (A and C) and bare (B and D) sediment. Rates are shown for the communities maintained at 25 °C at a 12 h L: 12 h D cycle (clear) and the communities maintained at 25 °C in darkness (black).

The isotopic signature of δ^{13}C-CH_4 decreased over time in both vegetated and bare sediments, whether they were maintained at constant temperature or experienced warming (Fig. 19). The isotopic signature in the vegetated sediment exposed to warming decreased significantly from -50.8 to -54.06 ‰ ($R^2 = 0.67$, $p < 0.001$).

The isotopic signature of the δ^{13}C-CO_2 became heavier with warming in the bare sediment, increasing from -22.36 at 25 °C to -9.01 ‰ at 37 °C ($R^2 = 0.91$, $p < 0.001$), while the other treatments showed similar average values of about -17 ‰ over time (Fig. 20).

The δ^{13}C isotopic composition of both CH_4 and CO_2 became heavier over time when the community was kept in the dark (Fig. 21), with a significant increase of δ^{13}C-CH_4 in the bare sediment ($R^2 = 0.94$, $p < 0.01$).

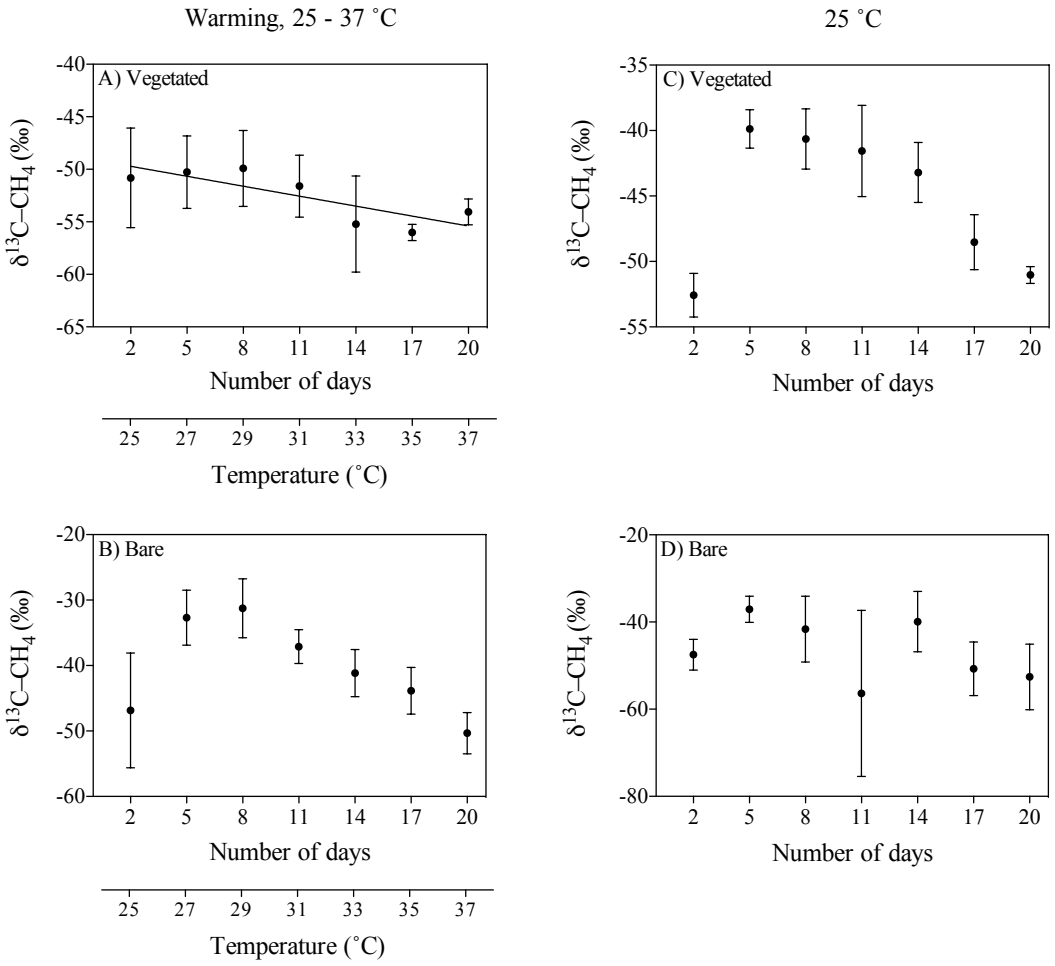

Figure 19: Mean ± SE isotopic signature of δ^{13}C-CH_4 in the communities experiencing warming from 25 - 37 °C (left) and the communities maintained at 25 °C (right). δ^{13}C-CH_4 is shown for the vegetated (A and C) and bare (B and D) sediment over the experimental period (number of days since sample collection). The second x-axis indicates the temperature increase for the community experiencing warming.

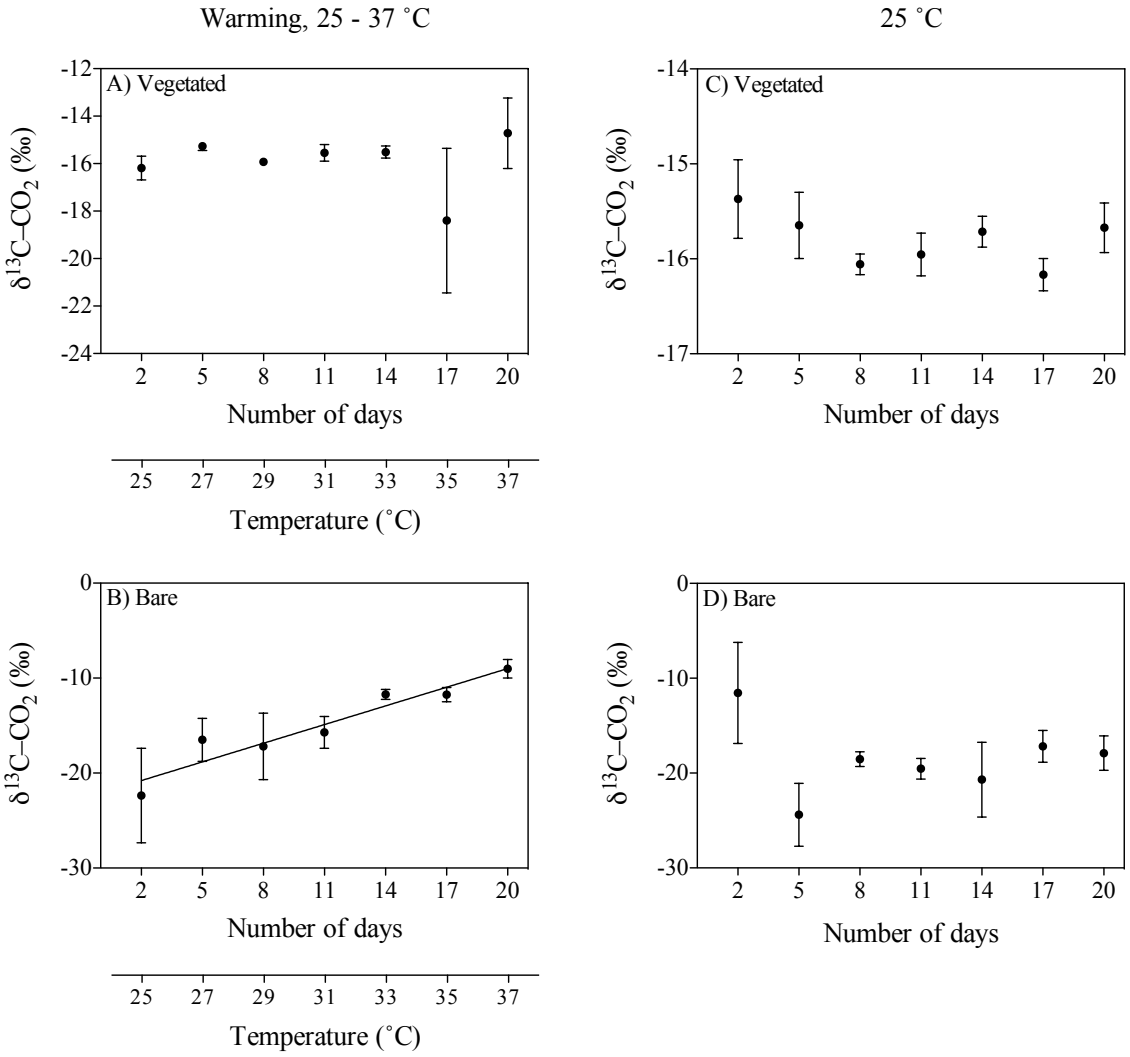

Figure 20: Mean ± SE isotopic signature of δ^{13}C-CO_2 in the communities experiencing warming from 25 - 37 °C (left) and the communities maintained at 25 °C (right). δ^{13}C-CO_2 is shown for the vegetated (A and C) and bare (B and D) sediment over the experimental period (number of days since sample collection). The second x-axis indicates the temperature increase for the community experiencing warming.

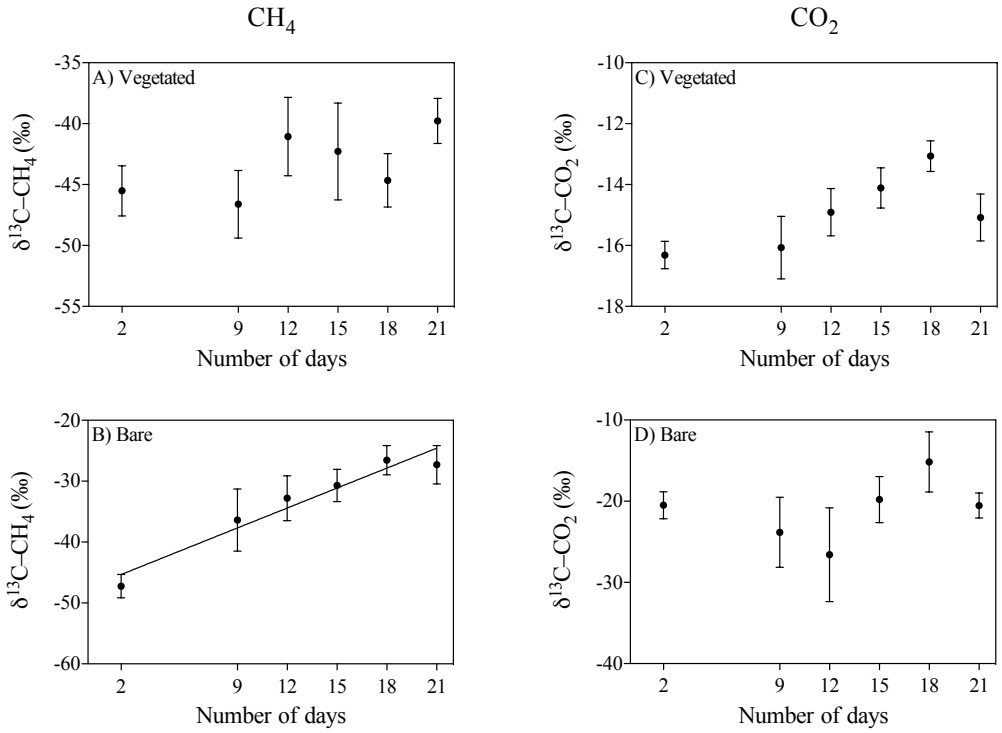

Figure 21: Mean ± SE isotopic signature of δ^{13}C-CH_4 (left) and δ^{13}C-CO_2 (right) in the vegetated (A and C) and bare (B and D) sediment of communitis kept in the dark.

3.3 Microbial community composition

The taxonomic composition of the archaeal communities revealed no distinct differences between different treatments and sample days (Fig. 22). The most abundant phyla were *Crenarchaeota* and *Eyryarchaeota*. The bacterial communities showed a similar trend with no clear differences between treatments and days (Fig. 23). All samplings were clearly dominated by *Proteobacteria*.

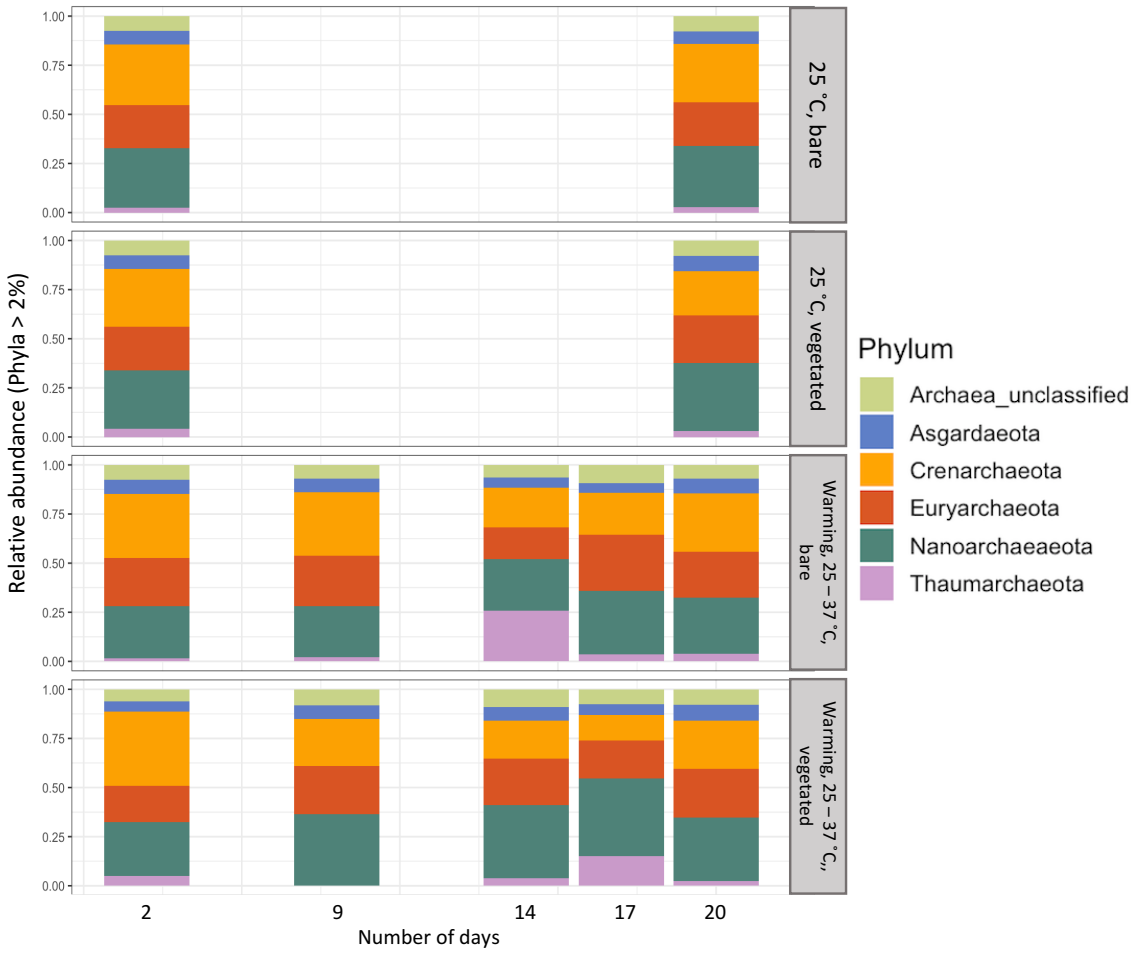

Figure 22: Archaeal community composition of the different treatments on the phyla level (abundance > 2%) over the experimental period (number of days since sample collection). Vegetated and bare sediments were analyzed with communities that were maintained at 25 °C, and communities experiencing warming from 25 - 37 °C.

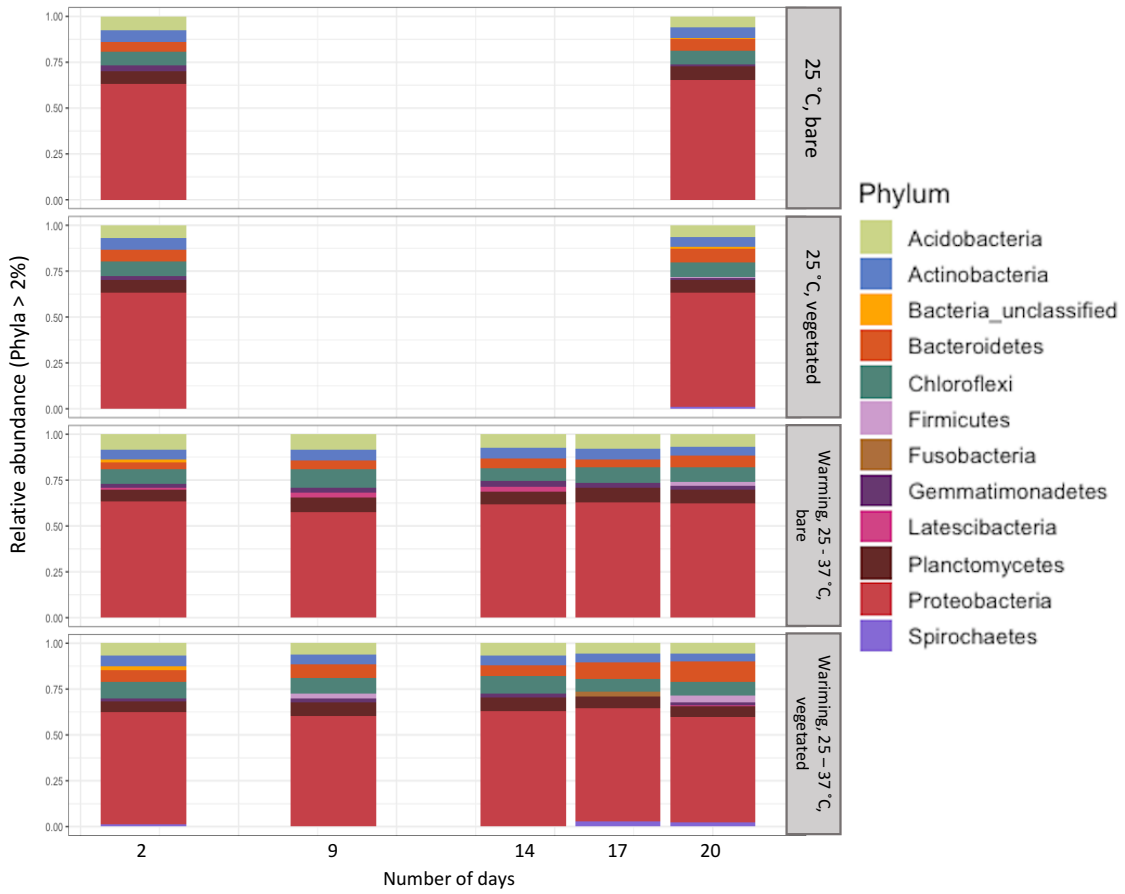

Figure 23: Bacterial community composition of the different treatments on the phyla level (abundance > 2%) over the experimental period (number of days since sample collection). Vegetated and bare sediments were analyzed with communities that were maintained at 25 °C, and communities experiencing warming from 25 - 37 °C.

These findings were also confirmed on the family level with no clear differences in the sediment microbiome between the sampling days and treatments (Fig. 24 and 25). The most dominant archaeal families in all treatments were *Marine Benthic Group D and DHVEG-1*, *Bathyarchaeia*, *Lokiarchaeia* and *Woesearchaeia* ranging between 12.82 - 14.29 % of all sequences. In the bacterial community, the most abundant families were *Woeseiaceae*, *Desulfobacteraceae*, *Thiotrichaceae* and *Gammaproteobacteria* (unclassified), *Actinomarinales* (uncultured) and *Pirellulaceae* ranging from 8.48 - 10.42 %. The composition of the vegetated sediment in the warming group on day 20, when temperature reached 37 °C, showed some differences compared to the other

treatments, with this community dominated by *Desulfobacteraceae* and *Gammaproteobacteria* (unclassified), and a higher diversity with 18 compared to 13 and 14 different families in vegetated sediment on day two and on day 20 when kept at 25 °C. Five families that were not aomong the most abundant families in any other sample were found here (*Marinifilaceae*, *Desulfovibrionaceae*, *Peptostreptococcaceae*, *GoM-GC232-4463-Bac1*, *Clostridiaceae 1*). However, the archaeal and bacterial communities seemed to differ between vegetated and bare sediments, particularly so for the archaeal community (Adonis permanova, $p < 0.05$, respectively; Fig. 26A), while there was no significant difference in the bacterial community (Adonis permanova, $p > 0.05$, respectively; Fig. 26B).

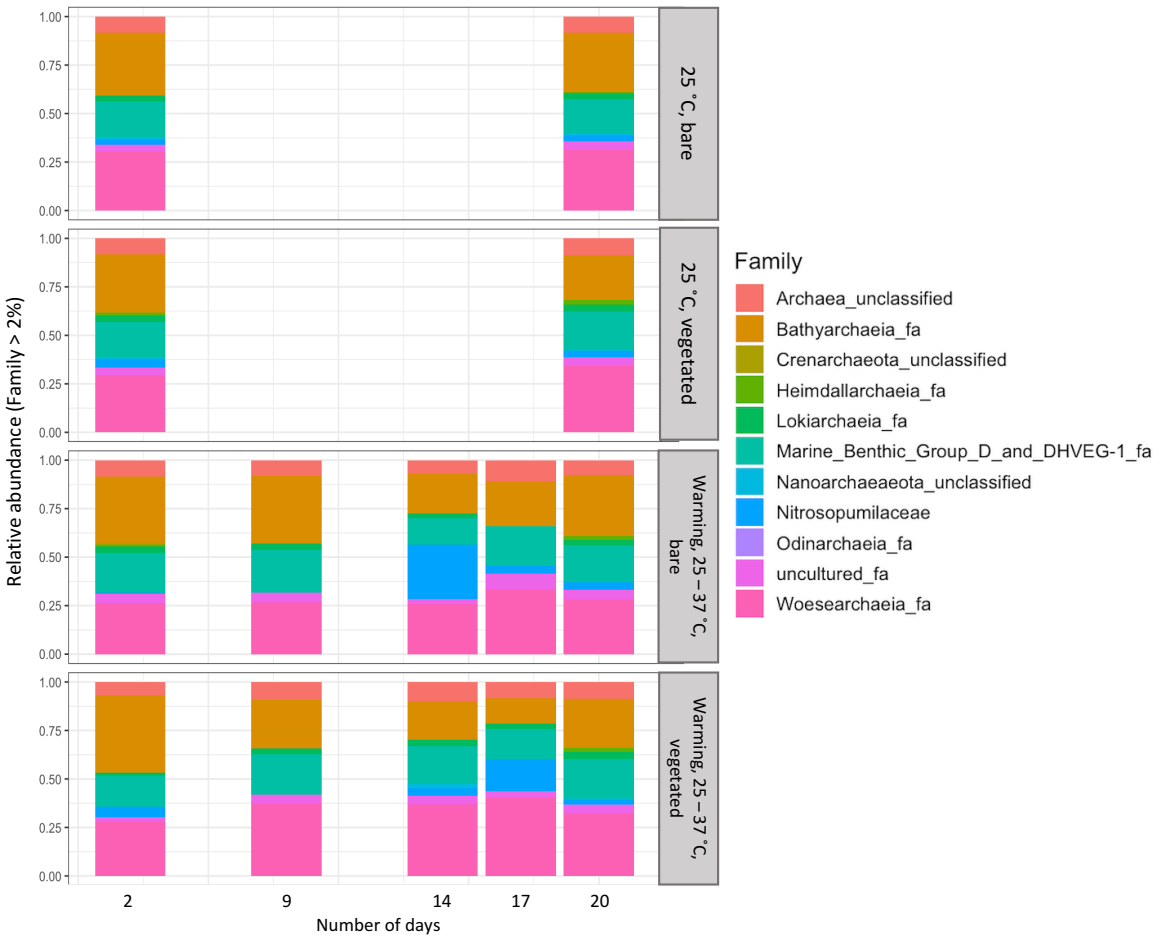

Figure 24: Archaeal community composition of the different treatments on the family level (abundance $> 2\%$) over the experimental period (number of days since sample collection). Vegetated and bare sediments were analyzed with communities that were maintained at 25 °C, and communities experiencing warming from 25 - 37 °C.

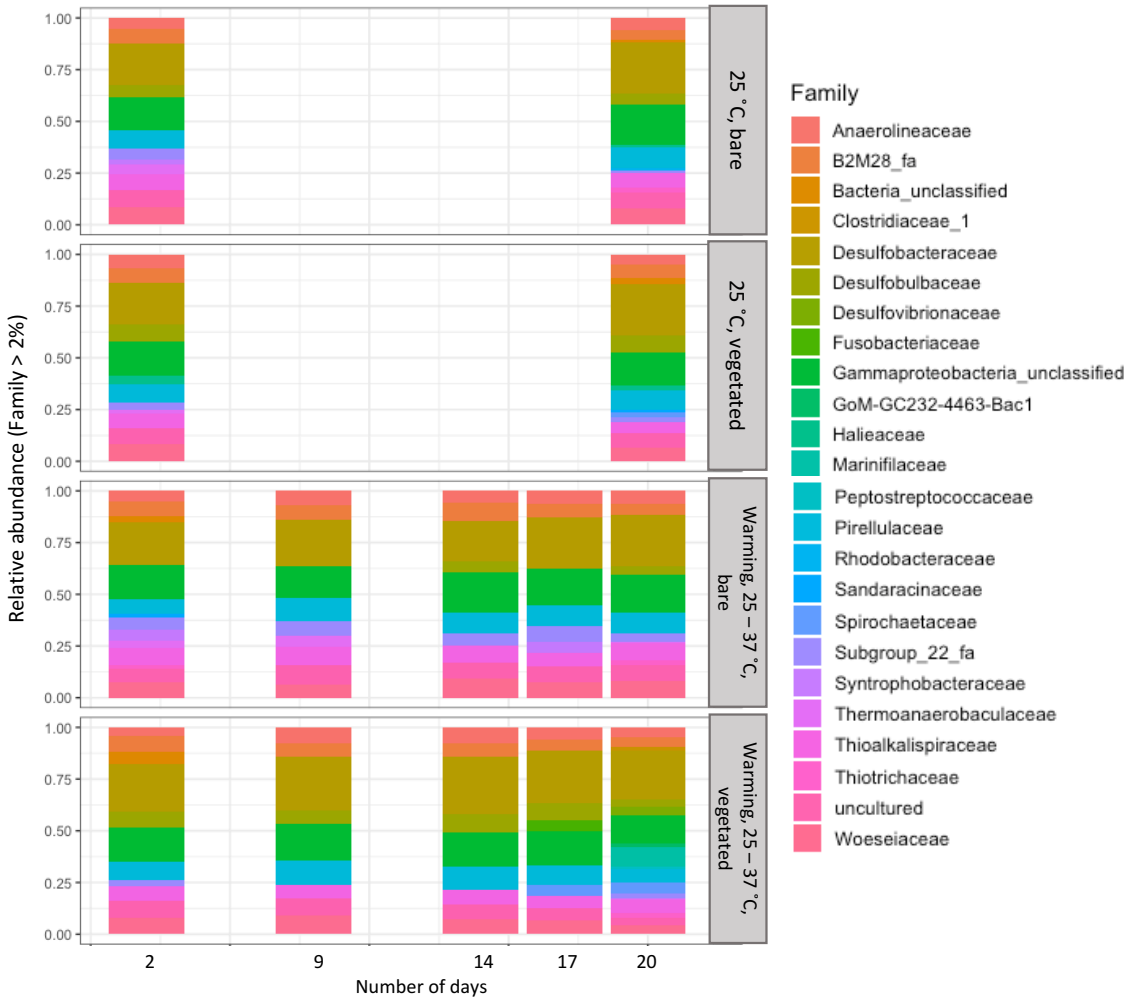

Figure 25: Bacterial community composition of the different treatments on the family level (abundance $> 2\%$) over the experimental period (number of days since sample collection). Vegetated and bare sediments were analyzed with communities that were maintained at 25 °C, and communities experiencing warming from 25 - 37 °C.

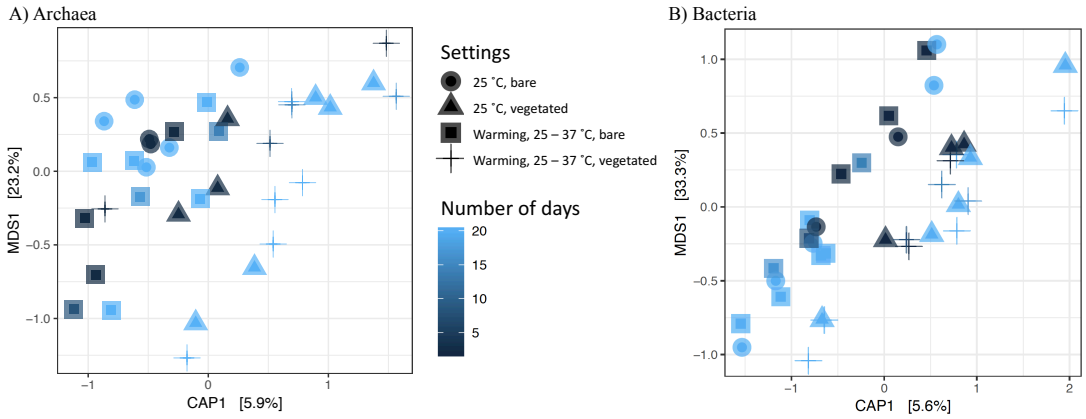

Figure 26: Multidimensional scaling (MDS) and constrained analysis of principal coordinates (CAP) to test for differences between the number of days since sample collection (day two: black, day 20: blue) and bare and vegetated sediments of communities maintained at 25 °C and communities experiencing warming 25 - 37 °C indicated by symbols. Plots show archaeal (A) and bacterial communities (B).

The archaeal community in vegetated sediments included a large core that was relatively unaffected by warming or incubation time, as the archaeal and bacterial communities at 25 °C shared about half of the OTUs (8,595 OTUs and 13,375 OTUs, respectively), with that sampled at 37 °C, after 20 days of continuous warming (Fig. 27 and 28). However, the number of OTUs, as well as alpha diversity of the sediment microbiome tended to increase over time regardless of warming, and did not show any consistent difference between bare and vegetated sediments (Fig. 29 and 30).

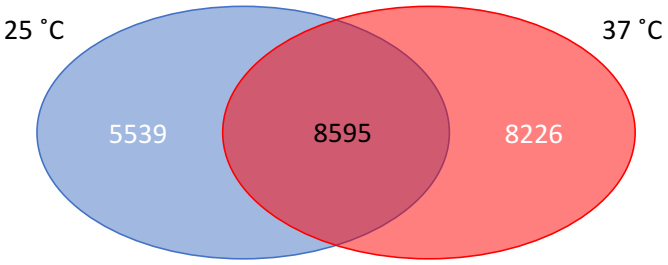

Figure 27: OTU counts of the archaeal community (abundance > 2%) in the vegetated sediment at 25 °C (blue) and in the vegetated sediment at 37 °C (red). The number in the middle represents shared OUT counts.

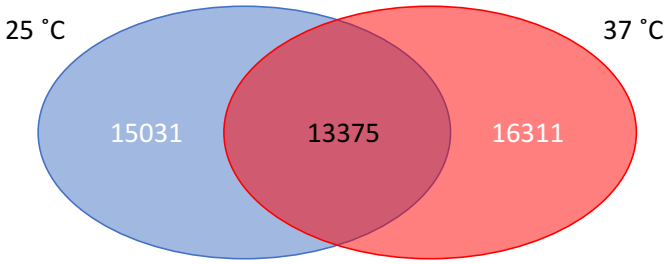

Figure 28: OTU counts of the bacterial community (abundance > 2%) in the vegetated sediment at 25 °C (blue) and in the vegetated sediment at 37 °C (red). The number in the middle represents shared OUT counts.

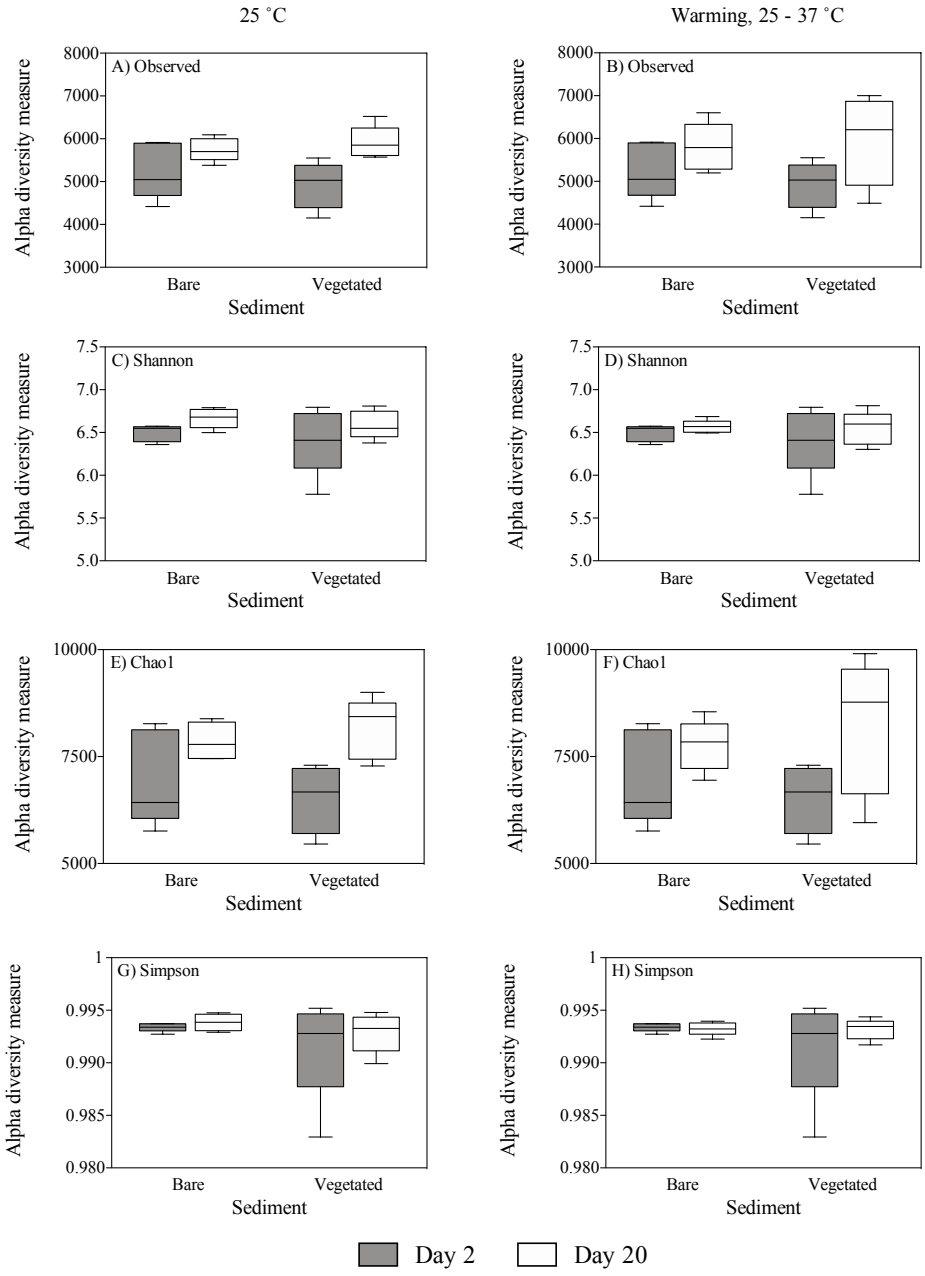

Figure 29: Alpha diversity measurements of the archaeal community based on observed OTUs (A and B), Shannon's index (C and D), Chao1 (E and F) and Simpson's index (G and H) in bare and vegetated sediments on day two (grey) and day 20 (white) after sample collection. Communities maintained at 25 °C (left) and communities experiencing warming from 25 -37 °C (right) are shown. Whiskers indicate 5 - 95 %.

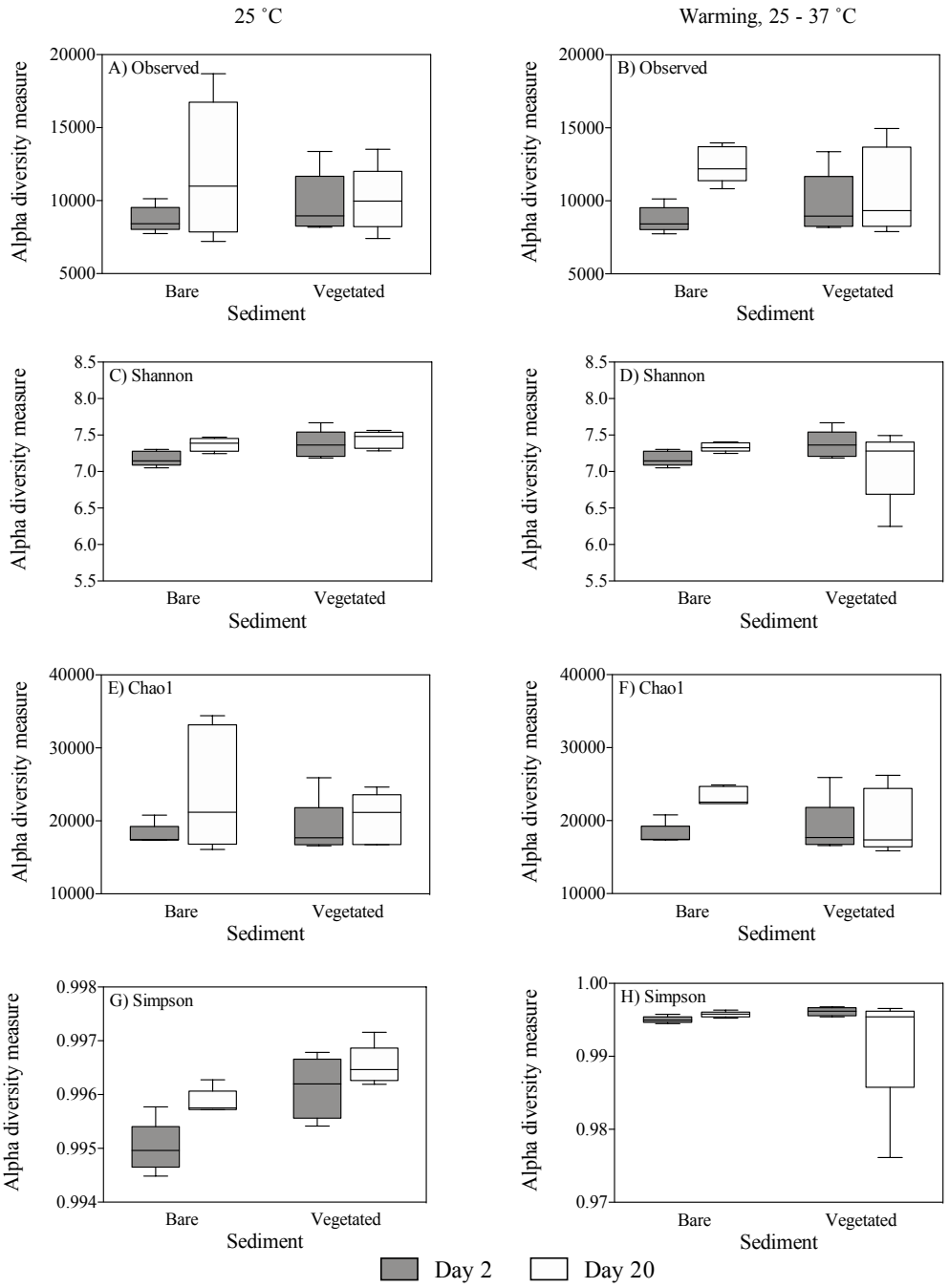

Figure 30: Alpha diversity measurements of the bacterial community based on observed OTUs (A and B), Shannon's index (C and D), Chao1 (E and F) and Simpson's index (G and H) in bare and vegetated sediments on day two (grey) and day 20 (white) after sample collection. Communities maintained at 25 °C (left) and communities experiencing warming from 25 -37 °C (right) are shown. Whiskers indicate 5 - 95 %.

4 Discussion

This study investigated the effects of increasing temperature on sediment-water fluxes of CH_4 and CO_2 by *H. stipulacea* sediments for the first time. In the Red Sea, Garcias-Bonet and Duarte (2017) found average CH_4 net production rates by seagrasses ranging from 1.4 (*Halophila decipiens*) to 401.3 µmol CH_4 m^{-2} d^{-1} (*Cymodocea serrulata* and *Halodule uninervis*), with an average rate of 61 µmol CH_4 m^{-2} d^{-1} in a mixed *H. stipulacea* and *H. uninervis* meadow. Similarly, net CH_4 production at the *in situ* temperature (25 °C) averaged 43.66 ± 8.36 µmol CH_4 m^{-2} d^{-1}. The slightly lower mean values compared to those reported by Garcias-Bonet and Duarte (2017) are accounted for by the decrease in fluxes over time in this study. In contrast, the community that was exposed to warming reached a maximum average of 88.11 ± 15.19 µmol CH_4 m^{-2} d^{-1} at 37 °C, which represents an increase of 377 % relative to the community held at 25 °C on the same incubation date. This clearly shows that temperature affects production rates, increasing the net production of CH_4, while rates decreased at a constant temperature. The increase in net production of CH_4 with warming is consistent with reports from Barber and Carlson (1993) for a *Thalassia testudinum* community in Florida Bay and Garcias-Bonet and Duarte (2017) for Red Sea seagrass communities, who reported higher production rates at higher temperatures. Even though we did see increased fluxes with warming, the values reported here are still within average rates reported for other seagrass species explained by variation between species and location. Previous studies on CH_4 production rates reported a large variation between greenhouse gas fluxes across species and locations (Table 3). These findings suggest high variability between different species and different locations, which may partially result from differences in ambient temperature

across sites and differences in composition as S4, the site with the highest organic matter content, shows higher greenhouse gas fluxes compared to S2, the site with the lowest content. Concurrently, S2 has the highest carbonate concentration while S4 has the lowest concentration. Similar trends were seen by Garcias-Bonet and Duarte (2017) who reported an increase in CH_4 production rates with increasing organic matter content in Red Sea seagrass sediments. They also reported decreasing rates with increasing distance from mainland which can also be associated to the sediment composition. These observations suggest that anthropogenic stressors resulting in increasing organic inputs to sediments, such as sewage discharge or eutrophication, can lead to higher CH_4 production rates.

Table 3: Mean CH_4 production rates reported in the literature and for the vegetated communities maintained at 25 °C in this study. The table was adapted from Garcias-Bonet and Duarte (2017).

Seagrass species	Location	Average CH_4 production (μmol CH_4 m^{-2} d^{-1})	References
Syringodium sp.	Bimini, Bahamas	5.8	Oremland, 1975
Thalassia testudinum	Florida, USA	44	Oremland, 1975
Thalassia testudinum	Florida, USA	183.4	Barber and Carlson, 1993
Enhalus acoroides	Sulawesi, Indonesia	118.8	Alongi et al., 2008
Zostera noltii	Arcachon Bay, France	98.4	Deborde et al., 2010
Zostera noltii	Ria Formosa, Portugal	307.2	Bahlmann et al., 2015
Halophila stipulacea and *Halodule uninervis*	Red Sea, Saudi Arabia	61	Garcias-Bonet and Duarte, 2017
Thalassodendron ciliatum	Red Sea, Saudi Arabia	3.2	Garcias-Bonet and Duarte, 2017
Thalassia hemprichii	Red Sea, Saudi Arabia	6.5	Garcias-Bonet and Duarte, 2017
Halophila decipiens	Red Sea, Saudi Arabia	1.4	Garcias-Bonet and Duarte, 2017
Enhalus acoroides	Red Sea, Saudi Arabia	96.2	Garcias-Bonet and Duarte, 2017
Cymodocea serrulata and *Halodule uninervis*	Red Sea, Saudi Arabia	401.3	Garcias-Bonet and Duarte, 2017
Halodule uninervis	Red Sea, Saudi Arabia	48.1	Garcias-Bonet and Duarte, 2017
Halodule sp. and *Halophila sp.*	Chilika, India	118	Banerjee et al., 2018
Halophila stipulacea	Red Sea, Saudi Arabia	43.7	This study

The differences between species do not only result from differences in their biomass or functions, but also from differences in the associated microbial community (Garcias-Bonet and Duarte, 2017). These variations can also be seen in this study as a high

variability is shown between the same seagrass species but different sites as well as within the same site. While the first set of measurements of the site S4 indicated CH_4 production rates of 400 - 500 µmol CH_4 m^{-2} d^{-1}, later measurements of communities sampled in the same meadow that were maintained at 25 °C showed 10-fold lower rates of around 50 µmol CH_4 m^{-2} d^{-1} and below, thereby revealing high variability in net CH_4 production rates over time.

Methane is produced under anoxic conditions in marine sediments. However, only a small portion is released, as CH_4 production by methanogens is compensated for by CH_4 consumption by sulfate-reducing bacteria (Barnes and Goldberg, 1976). However, the presence of seagrass results in a higher organic matter content favoring the presence of methanogens, which leads to higher CH_4 fluxes compared to those supported by adjacent bare sediments (Barber and Carlson, 1993; Bahlmann et al., 2015), consistent with the up to 100-fold higher CH_4 fluxes supported by vegetated compared to bare sediments in this study.

We found, however, no effect of prolonged darkness on CH_4 fluxes, suggesting that the elevated CH_4 fluxes in vegetated sediments are not directly supported by fresh photosynthetic products but rather by the elevated organic matter in vegetated sediments compared to bare ones. These findings are in contrast to those reported by Lyimo et al. (2018) who found increased CH_4 fluxes under shading, while the CH_4 fluxes decreased in this study.

CO_2 production rates revealed similar trends compared to the CH_4 production rates. There was also a high variability found between locations with rates up to four-fold higher in S4 compared to S2, and the vegetated sediment having up to six-fold higher rates compared to bare sediment.

CO_2 production rates increased with warming, while the rates of communities maintained at 25 °C stayed rather constant in the bare sediment and slightly decreased

in the vegetated sediment. Rates reported in a mixed *Halodule sp.* and *Halophila sp.* meadow in India (980 µmol CO_2 m^{-2} d^{-1}; Banerjee et al. (2018)) are about three-fold higher compared to rates found in vegetated sediments maintained at 25 °C. With warming, the communities shifted to acting as a carbon source, while communities at a constant 25 °C seemed to continue CO_2 consumption in both the vegetated and bare sediment. Warming increases respiration at higher rates than photosynthesis (Harris et al., 2006) and both photosynthesis and respiration increase up to a thermal optimum (Marsh et al., 1986). While photosynthesis decreases past the optimum, respiration continues to increase (Marsh et al., 1986) leading to an imbalance in the carbon cycle.

Communities that were maintained at 25 °C and a 12 h L : 12 h D photoperiod showed continuous net CO_2 consumption, while the communities kept in darkness shifted to a heterotrophic system, acting as a CO_2 source, with the net CO_2 production corresponding to community respiration rates, while that at 12 h L : 12 h D photoperiod corresponded to the net community production. Blue carbon ecosystems have shown to turn into carbon sources when disturbances lead to mortality (Macreadie et al., 2015; Lovelock et al., 2017; Arias-Ortiz et al., 2018). In this study, this was especially apparent with an outlier at 33 °C in the vegetated sediment, where we detected net CH_4 production rates of 699.81 µmol CH_4 m^{-2} d^{-1} and net CO_2 production of 55,169.49 µmol CO_2 m^{-2} d^{-1}. At this point, the seagrass community inside this core was already dead, while the seagrass in other cores held at similar temperatures were only showing first signs of mortality. We can therefore assume that mortality caused by warming might lead to the release of sequestered carbon turning seagrass meadows into carbon sources.

Converting these values into CO_2 equivalents, taking into account the GWP for CH_4 on a 100 year time scale (28; Myhre et al. (2013)), the production rates in the vegetated sediment increased from 2262.47 to 12,889.16 µmol CO_2e m^{-2} d^{-1} under

warming with CO_2 being the main source. In contrast, in the community maintained at 25 °C, the consumption rate was -425.11 ± 197.61 µmol CO_2e m^{-2} d^{-1} on the last day of incubation. While these communities showed net CO_2e production rates at the beginning of the experiment, the system shifted to being a carbon sink on day 14. Mean values for the entire experimental period revealed that only the bare sediment maintained at 25 °C seemed to act as a carbon sink (-20.55 ± 91.73 µmol CO_2e m^{-2} d^{-1}), while the vegetated and bare sediments exposed to warming showed CO_2e production rates ranging from 740.8 ± 405 (vegetated maintained at 25 °C) to 4718 ± 1586 µmol CO_2e m^{-2} d^{-1} (vegetated experiencing warming).

In this study, the isotopic signature of the CO_2 released from bare sediments shifted from -22.36 to -9.01 ‰ with warming indicating a shift from seston (-25.43 ± 0.42 ‰; Duarte et al. (2018b)) as the organic matter supporting respiration to seagrass (average δ^{13}C value of -7.73 ± 0.11 ‰ for Red Sea seagrass (Duarte et al., 2018b) as a source. Serrano et al. (2018) reported similar values with an average δ^{13}C of -14.55 ± 0.24 ‰ in soil organic matter of a *H. stipulacea* meadow in Al Kharar. In the vegetated cores, the isotopic composition stayed rather constant indicating seagrass to be the main organic carbon source regardless of warming.

There is also a shift seen in the source of carbon supporting CH_4 fluxes. Biogenic sources usually have a lighter isotopic signature (-40 to -80 ‰) compared to thermogenic sources (-30 to -50 ‰; Reeburgh (2003)). Additionally, there is also a shift to lighter values due to methanogensis, while methanotrophy leads to a heavier isotopic signature (Whiticar, 1990). In this study, we found a shift to a lighter isotopic signature indicating an increasing CH_4 production by methanogens.

Generally, the sediment microbiome seemed to be similar between vegetated and bare sediments and rather resilient to changes in temperature. Similar findings were

reported for the bacterial composition in a *Zostera muelleri* sediment in Australia, which was exposed to warming from 23 to 30 °C (Trevathan-Tackett et al., 2017). The same trend was found in sulfate-reducing bacteria in temperate sediments, while the abundance declined in Arctic sediments with warming (Robador et al., 2009). While this could imply that temperate bacterial communities are already adapted to seasonal temperature changes (Robador et al., 2009), we can also assume that microbial communities in the Red Sea might already be adapted to higher temperatures. In contrast, other disturbances such as elevated pCO_2 have shown to shift the microbial community composition in seagrasses (Hassenrück et al., 2015). In other organisms such as corals, microbial communities have also shown to shift during coral bleaching induced by warming (Bourne et al., 2008). Elevated temperatures also led to a tendency for diversity to increase in disturbed corals as they are less resilient to microbes which would not be found in corals under normal conditions (McDevitt-Irwin et al., 2017). A similar effect was seen in this the bacterial community, as we found an increased number (18) of the most abundant families in the communities that experienced warming compared to 12 - 15 families in bare sediments and at 25 °C. There were five families (abundance $>$ 2 %) at 37 °C in vegetated sediments that were not among the most abundant families in any other sample (*Marinifilaceae*, *Desulfovibrionaceae*, *Peptostreptococcaceae*, *GoM-GC232-4463-Bac1*, *Clostridiaceae 1*), indicating that there is an increase in diversity at higher temperatures. This correlates with the increased CH_4 and CO_2 fluxes indicating that the warming affects both the microbiome diversity and greenhouse gas fluxes.

The bacterial community composition was dominated by the phylum *Proteobacteria*, which has been identified as the most abundant phylum above and belowground in other *H. stipulacea* communites in the Red Sea (Weidner et al., 2000; Meija et al., 2016), as well as in the microbiome of other seagrass species (Cúcio et al., 2016; Fraser et al., 2018). Unclassified *Gammaproteobacteria* and *Desulfobacteraceae* were

the most abundant families (up to 10.42 % of the sequences > 2 %), and they were also found in other seagrass species as they play an important role in the sulfur metabolism (Cúcio et al., 2016, 2018). Fraser et al. (2018) found a high abundance of genes involved in the sulfur cycle in seagrass meadows indicating that this might not be restrictive to specific seagrass species or locations. These findings confirm the importance of the sulfur cycle in seagrass sediments, as sulfate-reducing and sulfur-oxidizing bacteria are highly abundant in the rhizosphere of seagrasses (Cifuentes et al., 2000; Cúcio et al., 2016).

Two of the most dominant archaeal phyla found in all samples, *Crenarchaeota* and *Euryarchaeota* were also found in Arctic methane-containing permafrost (Shcherbakova et al., 2016), and were also reported in sediments of a *Zostera noltii* meadow (Cifuentes et al., 2000). Even though methanogens belong to the phylum *Euryarchaeota*, methanogens were not part of the most abundant families found in this study. However, the most abundant families found in this study still play a role in methane prodcution. In addition to methanogens, Evans et al. (2015) reported that the phylum *Bathyarchaeota* also contributes to the methane cycle, and *Bathyarchaeia_fa* was one of the most abundant families in our samples (up to 13.89 %). *Woesearchaeia*, another abundant family in all samples (up to 13.89 %), are part of the carbon metabolism under anoxic conditions (Castelle et al., 2015). Additionally, *Woesearchaeia* are believed to provide acetate and hydrogen to methanogens supporting their growth, while *Woesearchaeia* might benefit by receiving compounds to compensate for their metabolic deficiencies (Liu et al., 2018). These families might therefore play a role in the methane production, yet none of these families changed in their abundance with warming nor their abundance (as number of reads) showed any correlation to CH_4 or CO_2 gas fluxes. However, even though the most abundant phyla and families were rather stable, significant differences between the sampling times reveal that there must be differences in the less abundant families and genera.

Conclusion

This study presents, for the first time, the effect of increasing temperature on greenhouse gas production rates by *H. stipulacaea* in the Red Sea. Warming led to an increase in CH_4 and CO_2 fluxes, and vegetated sediments experienced higher fluxes compared to bare sediments, with seagrass mortality shown to trigger very high CH_4 and CO_2 production. Additionally, a higher organic matter content was associated with elevated CH_4 and CO_2 fluxes. However, we did not observe any clear changes in the microbial community composition with warming. The sediment microbiome, as represented by archaeal and bacterial communities, seemed to be resilient to warming and stayed rather stable. The isotopic signature of CH_4 and CO_2 was partly affected by increasing temperatures as $\delta^{13}C$ supporting CO_2 stayed rather stable in vegetated sediments over time, while the sources seemed to shift towards seagrass as a source of carbon in bare sediments. $\delta^{13}C$ supporting CH_4 shifted to lighter values indicating the biogenic source of CH_4. Even though methanogens were not among the most abundant taxa in the microbial communities, the isotopic signature is an indication that methanogenesis is fueled by higher temperatures. We could also show that the effects seen were caused by increasing temperatures as we did not detect similar rates when seagrass was kept in darkness. Even though the photosynthesis was suppressed, which ultimately led to mortality, the rates of greenhouse gas production did not increase but rather decreased in the case of CH_4. However, both disturbances led to the release of sequestered carbon. This indicates that blue carbon ecosystems are under threat by disturbances and especially climate change, and action needs to be taken to protect these valuable ecosystems. These findings have critical implications when predicting future changes in the atmospheric CH_4 and CO_2 concentrations. Increased greenhouse gas production rates by disturbed seagrass meadows may contribute to

emissions through “land use change”.

REFERENCES

Albritton, D. L., Meira Filho, L., Cubasch, U., Dai, X., Ding, Y., Griggs, D., Hewitson, B., Houghton, J., Isaksen, I., Karl, T., McFarland, M., Meleshko, V., Mitchell, J., Noguer, M., Nyenzi, B., Oppenheimer, M., Penner, J., Pollonais, S., Stocker, T., and Trenberth, K. (2001). Technical Summary. In Houghton, J., Ding, Y., Griggs, D., Noguer, M., van der Linden, P., Dai, X., Maskell, K., and Johnson, C., editors, *Climate Change 2001: The Scientific Basis. Contribution of Working Group I to the Third Assessment Report of the Intergovernmental Panel on Climate Change*, page 881. Cambridge, United Kingdom and New York, NY, USA.

Allison, E. H., Perry, A. L., Badjeck, M.-C., Adger, W. N., Brown, K., Conway, D., Halls, A. S., Pilling, G. M., Reynolds, J. D., Andrew, N. L., and Dulvy, N. K. (2009). Vulnerability of national economies to the impacts of climate change on fisheries. *Fish and Fisheries*, 10(2):173–196.

Alongi, D. M., Trott, L., Undu, M. C., and Tirendi, F. (2008). Benthic microbial metabolism in seagrass meadows along a carbonate gradient in Sulawesi, Indonesia. *Aquatic Microbial Ecology*, 51:141–152.

Arias-Ortiz, A., Serrano, O., Masqué, P., Lavery, P. S., Mueller, U., Kendrick, G. A., Rozaimi, M., Esteban, A., Fourqurean, J. W., Marbà, N., Mateo, M. A., Murray, K., Rule, M. J., and Duarte, C. M. (2018). A marine heatwave drives massive losses from the world's largest seagrass carbon stocks. *Nature Climate Change*, 8(4):338–344.

Bahlmann, E., Weinberg, I., Lavrič, J. V., Eckhardt, T., Michaelis, W., Santos, R., and Seifert, R. (2015). Tidal controls on trace gas dynamics in a seagrass meadow of the Ria Formosa lagoon (southern Portugal). *Biogeosciences*, 12:1683–1696.

Banerjee, K., Paneerselvam, A., Ramachandran, P., Ganguly, D., Singh, G., and Ramesh, R. (2018). Seagrass and macrophyte mediated CO_2 and CH_4 dynamics in shallow coastal waters. *Plos One*, 13(10):e0203922.

Barber, T. R. and Carlson, P. R. J. (1993). Effects of Seagrass Die-Off on Benthic Fluxes and Porewater Concentrations of $\sum CO_2$, $\sum H_2S$, and CH_4 in Florida Bay

Sediments. In *Biogeochemistry of Global Change*, pages 530–550. Springer US, Boston, MA.

Barnes, R. O. and Goldberg, E. D. (1976). Methane production and consumption in anoxic marine sediments. *Geology*, 4(5):297–300.

Bolger, A. M., Lohse, M., and Usadel, B. (2014). Trimmomatic: A flexible trimmer for Illumina Sequence Data. *Bioinformatics*, btu170.

Bourne, D., Iida, Y., Uthicke, S., and Smith-Keune, C. (2008). Changes in coral-associated microbial communities during a bleaching event. *ISME Journal*, 2:350–363.

Castelle, C. J., Wrighton, K. C., Thomas, B. C., Hug, L. A., Brown, C. T., Wilkins, M. J., Frischkorn, K. R., Tringe, S. G., Singh, A., Markillie, L. M., Taylor, R. C., Williams, K. H., and Banfiel, J. F. (2015). Genomic Expansion of Domain Archaea Highlights Roles for Organisms from New Phyla in Anaerobic Carbon Cycling. *Current Biology*, 25:690–701.

Cifuentes, A., Antón, J., Benlloch, S., Donnelly, A., Herbert, R. A., and Rodríguez-Valera, F. (2000). Prokaryotic diversity in Zostera noltii-colonized marine sediments. *Applied and Environmental Microbiology*, 66(4):1715–1719.

Collier, C. J. and Waycott, M. (2014). Temperature extremes reduce seagrass growth and induce mortality. *Marine Pollution Bulletin*, 83(2):483–490.

Collins, M., Knutti, R., Arblaster, J., Dufresne, J.-L., Fichefet, T., Friedlingstein, P., Gao, X., Gutowski, W. J., Johns, T., Krinner, G., Shongwe, M., Tebaldi, C., Weaver, A. J., and Wehner, M. (2013). Long-term Climate Change: Projections, Commitments and Irreversibility. *Climate Change 2013: The Physical Science Basis. Contribution of Working Group I to the Fifth Assessment Report of the Intergovernmental Panel on Climate Change*, pages 1029–1136.

Costanza, R., D'Arge, R., de Groot, R., Farber, S., Grasso, M., Hannon, B., Limburg, K., Naeem, S., O'Neill, R. V., Paruelo, J., Raskin, R. G., Sutton, P., and van den Belt, M. (1997). The value of the world's ecosystem services and natural capital. *Nature*, 387(6630):253–260.

Cúcio, C., Engelen, A. H., Costa, R., and Muyzer, G. (2016). Rhizosphere microbiomes of European seagrasses are selected by the plant, but are not species specific. *Frontiers in Microbiology*, 7(440):1–15.

Cúcio, C., Overmars, L., Engelen, A. H., and Muyzer, G. (2018). Metagenomic Analysis Shows the Presence of Bacteria Related to Free-Living Forms of Sulfur-Oxidizing Chemolithoautotrophic Symbionts in the Rhizosphere of the Seagrass Zostera marina. *Frontiers in Marine Science*, 5(May):1–15.

Deborde, J., Anschutz, P., Guérin, F., Poirier, D., Marty, D., Boucher, G., Thouzeau, G., Canton, M., and Abril, G. (2010). Methane sources, sinks and fluxes in a temperate tidal Lagoon: The Arcachon lagoon (SW France). *Estuarine, Coastal and Shelf Science*, 89:256–266.

Duarte, B., Martins, I., Rosa, R., Matos, A. R., Roleda, M. Y., Reusch, T., Engelen, A. H., Serrao, E. A., Pearson, G. A., Marques, J. C., Caçador, I., Duarte, C. M., and Jüterbock, A. (2018a). Climate change impacts on seagrass meadows and macroalgal forests: an integrative perspective on acclimation and adaptation potential. *Frontiers in Marine Science*, 5:190.

Duarte, C. M. (1995). Submerged aquatic vegetation in relation to different nutrient regimes. *Ophelia*, 41(1):87–112.

Duarte, C. M., Delgado-Huertas, A., Anton, A., Carrillo-de Albornoz, P., López-Sandoval, D. C., Agustí, S., Almahasheer, H., Marbá, N., Hendriks, I. E., Krause-Jensen, D., and Garcias-Bonet, N. (2018b). Stable Isotope (δ^{13}C, δ^{15}N, δ^{18}O, δD) Composition and Nutrient Concentration of Red Sea Primary Producers. *Frontiers in Marine Science*, 5(August):1–12.

Duarte, C. M., Holmer, M., and Marbà, N. (2013). Plant-Microbe Interactions in Seagrass Meadows. In Kristensen, E., Haese, R. R., and Kostka, J. E., editors, *Interactions Between Macro- and Microorganisms in Marine Sediments, Volume 60*, pages 31–60.

Duarte, C. M., Marbà, N., Gacia, E., Fourqurean, J. W., Beggins, J., Barrón, C., and Apostolaki, E. T. (2010). Seagrass community metabolism: Assessing the carbon sink capacity of seagrass meadows. *Global Biogeochemical Cycles*, 24(4):1–9.

Duarte, C. M., Middelburg, J. J., and Caraco, N. (2005). Major role of marine vegetation on the oceanic carbon cycle. *Biogeosciences*, 2:1–8.

El Shaffai, A. (2016). *Field Guide to Seagrasses of the Red Sea*. Gland, Switzerland: IUCN and Courbevoie, France: Total Foundation, first edition.

Enríquez, S., Duarte, C. M., and Sand-Jensen, K. (1993). Patterns in decomposition rates among photosynthetic organisms: the importance of detritus C:N:P content. *Oecologia*, 94(4):457–471.

Evans, P. N., Parks, D. H., Chadwick, G. L., Robbins, S. J., Orphan, V. J., Golding, S. D., and Tyson, G. W. (2015). Methane metabolism in the archaeal phylum Bathyarchaeota revealed by genome-centric metagenomics. *Science*, 350(6259):434–438.

Fourqurean, J. W., Duarte, C. M., Kennedy, H., Marbà, N., Holmer, M., Mateo, M. A., Apostolaki, E. T., Kendrick, G. A., Krause-Jensen, D., McGlathery, K. J., and Serrano, O. (2012a). Seagrass ecosystems as a globally significant carbon stock. *Nature Geoscience*, 5(7):505–509.

Fourqurean, J. W., Kendrick, G. A., Collins, L. S., Chambers, R. M., and Vanderklift, M. A. (2012b). Carbon, nitrogen and phosphorus storage in subtropical seagrass meadows: Examples from Florida Bay and Shark Bay. *Marine and Freshwater Research*, 63(11):967–983.

Fourqurean, J. W., Powell, G. V. N., Kenworthy, W. J., and Zieman, J. C. (1995). The effects of long-term manipulation of nutrient supply on competition between the seagrasses Thalassia testudinum and Halodule wrightii in Florida Bay. *Oikos*, 72(3):349–358.

Fraser, M. W., Gleeson, D. B., Grierson, P. F., Laverock, B., and Kendrick, G. A. (2018). Metagenomic Evidence of Microbial Community Responsiveness to Phosphorus and Salinity Gradients in Seagrass Sediments. *Frontiers in Microbiology*, 9(1703):1–11.

Garcias-Bonet, N. and Duarte, C. M. (2017). Methane Production by Seagrass Ecosystems in the Red Sea. *Frontiers in Marine Science*, 4(340):1–10.

Gerloff, G. C. and Krombholz, P. H. (1966). Tissue Analysis As a Measure of Nutrient Availability for the Growth of Angiosperm Aquatic Plants. *Limnology and Oceanography*, 11(4):529–537.

Gonsalves, M. J., Fernandes, C. E., Fernandes, S. O., Kirchman, D. L., and Loka Bharathi, P. A. (2011). Effects of composition of labile organic matter on biogenic production of methane in the coastal sediments of the Arabian Sea. *Environmental Monitoring and Assessment*, 182(1-4):385–395.

Harris, L. A., Duarte, C. M., and Nixon, S. W. (2006). Allometric Laws and Prediction in Esturine and Costal Ecology. *Estuaries and Coasts*, 29(2):340–344.

Hassenrück, C., Hofmann, L. C., Bischof, K., and Ramette, A. (2015). Seagrass biofilm communities at a naturally CO_2-rich vent. *Environmental Microbiology Reports*, 7(3):516–525.

Hoegh-Guldberg, O. (1999). Environmental and economic importance of the world's coral reefs. *Marine and Freshwater Research*, 50:839–866.

Hoegh-Guldberg, O. and Bruno, J. F. (2010). The Impact of Climate Change on the World's Marine Ecosystems. *Science*, 328(5985):1523–1529.

IPCC (2014). Climate Change 2014: Synthesis Report. Contribution of Working Groups I, II and III to the Fifth Assessment Report of the Intergovernmental Panel on Climate Change. page 151. IPCC, Geneva, Switzerland.

Joos, F., Plattner, G.-K., Stocker, T. F., Marchal, O., and Schmittner, A. (1999). Global Warming and Marine Carbon Cycle Feedbacks on Future Atmospheric CO_2. *Science*, 284(5413):464–467.

Kirschke, S., Bousquet, P., Ciais, P., Saunois, M., Canadell, J. G., Dlugokencky, E. J., Bergamaschi, P., Bergmann, D., Blake, D. R., Bruhwiler, L., Cameron-Smith, P., Castaldi, S., Chevallier, F., Feng, L., Fraser, A., Heimann, M., Hodson, E. L., Houweling, S., Josse, B., Fraser, P. J., Krummel, P. B., Lamarque, J. F., Langenfelds, R. L., Le Quéré, C., Naik, V., O'doherty, S., Palmer, P. I., Pison, I., Plummer, D., Poulter, B., Prinn, R. G., Rigby, M., Ringeval, B., Santini, M., Schmidt, M., Shindell, D. T., Simpson, I. J., Spahni, R., Steele, L. P., Strode, S. A., Sudo, K., Szopa, S., Van Der Werf, G. R., Voulgarakis, A., Van Weele, M., Weiss, R. F., Williams, J. E., and Zeng, G. (2013). Three decades of global methane sources and sinks. *Nature Geoscience*, 6:813–823.

Krause-Jensen, D., Serrano, O., Apostolaki, E. T., Gregory, D. J., and Duarte, C. M. (2018). Seagrass sedimentary deposits as security vaults and time capsules of the human past. *Ambio*, pages 1–11.

Lamb, J. B., Van De Water, J. A., Bourne, D. G., Altier, C., Hein, M. Y., Fiorenza, E. A., Abu, N., Jompa, J., and Harvell, C. D. (2017). Seagrass ecosystems reduce exposure to bacterial pathogens of humans, fishes, and invertebrates. *Science*, 355(6326):731–733.

Le Quéré, C., Raupach, M. R., Canadell, J. G., Marland, G., Bopp, L., Ciais, P., Conway, T. J., Doney, S. C., Feely, R. A., Foster, P., Friedlingstein, P., Gurney, K., Houghton, R. A., House, J. I., Huntingford, C., Levy, P. E., Lomas, M. R., Majkut, J., Metzl, N., Ometto, J. P., Peters, G. P., Prentice, I. C., Randerson, J. T., Running, S. W., Sarmiento, J. L., Schuster, U., Sitch, S., Takahashi, T., Viovy, N., van der Werf, G. R., and Woodward, F. I. (2009). Trends in the sources and sinks of carbon dioxide. *Nature Geoscience*, 2:831–836.

Ledley, T. S., Sundquist, E. T., Schwartz, S. E., Hall, D. K., Fellows, J. D., and Killeen, T. L. (1999). Climate change and greenhouse gases. *Eos*, 80(39):453–458.

Lipkin, Y. (1975). Halophila stipulacea, a review of a successful immigration. *Aquatic Botany*, 1:203–215.

Liu, X., Li, M., Castelle, C. J., Probst, A. J., Zhou, Z., Pan, J., Liu, Y., Banfield, J. F., and Gu, J. D. (2018). Insights into the ecology, evolution, and metabolism of the widespread Woesearchaeotal lineages. *Microbiome*, 6(1):1–16.

Liu, Y. and Whitman, W. B. (2008). Metabolic, phylogenetic, and ecological diversity of the methanogenic archaea. *Annals of the New York Academy of Sciences*, 1125:171–189.

Lovelock, C. E., Atwood, T., Baldock, J., Duarte, C. M., Hickey, S., Lavery, P. S., Masque, P., Macreadie, P. I., Ricart, A. M., Serrano, O., and Steven, A. (2017). Assessing the risk of carbon dioxide emissions from blue carbon ecosystems. *Frontiers in Ecology and the Environment*, 15(5):257–265.

Lyimo, L. D., Gullström, M., Lyimo, T. J., Deyanova, D., Dahl, M., Hamisi, M. I., and Björk, M. (2018). Shading and simulated grazing increase the sulphide pool and methane emission in a tropical seagrass meadow. *Marine Pollution Bulletin*, 134:89–93.

Macreadie, P. I., Trevathan-Tackett, S. M., Skilbeck, C. G., Sanderman, J., Curlevski, N., Jacobsen, G., and Seymour, J. R. (2015). Losses and recovery of organic carbon from a seagrass ecosystem following disturbance. *Proceedings of the Royal Society B: Biological Sciences*, 282:1–6.

Marbà, N., Arias-Ortiz, A., Masqué, P., Kendrick, G. A., Mazarrasa, I., Bastyan, G. R., Garcia-Orellana, J., and Duarte, C. M. (2015). Impact of seagrass loss and

subsequent revegetation on carbon sequestration and stocks. *Journal of Ecology*, 103(2):296–302.

Marbà, N. and Duarte, C. M. (2010). Mediterranean warming triggers seagrass (Posidonia oceanica) shoot mortality. *Global Change Biology*, 16(8):2366–2375.

Marsh, J. A., Dennison, W. C., and Alberte, R. S. (1986). Effects of temperature on photosynthesis and respiration in eelgrass (Zostera marina L.). *Journal of Experimental Marine Biology and Ecology*, 101:257–267.

Mateo, M. A., Romero, J., Pérez, M., Littler, M. M., and Littler, D. S. (1997). Dynamics of millenary organic deposits resulting from the growth of the Mediterranean seagrass Posidonia oceanica. *Estuarine, Coastal and Shelf Science*, 44:103–110.

McDevitt-Irwin, J. M., Baum, J. K., Garren, M., and Vega Thurber, R. L. (2017). Responses of Coral-Associated Bacterial Communities to Local and Global Stressors. *Frontiers in Marine Science*, 4(262):1–16.

McLeod, E., Chmura, G. L., Bouillon, S., Salm, R., Björk, M., Duarte, C. M., Lovelock, C. E., Schlesinger, W. H., and Silliman, B. R. (2011). A blueprint for blue carbon: Toward an improved understanding of the role of vegetated coastal habitats in sequestering CO2. *Frontiers in Ecology and the Environment*, 9(10):552–560.

McManus, J. W. and Polsenberg, J. F. (2004). Coral-algal phase shifts on coral reefs: Ecological and environmental aspects. *Progress in Oceanography*, 60(2-4):263–279.

McMurdie, P. and Holmes, S. (2013). phyloseq: An R package for reproducible interactive analysis and graphics of microbiome census data. *PLoS ONE*, 8(4):e61217.

Meija, A. Y., Rotini, A., Lacasella, F., Bookman, R., Thaller, M. C., Shem-Tov, R., Winters, G., and Migliore, L. (2016). Assessing the ecological status of seagrasses using morphology, biochemical descriptors and microbial community analyses. A study in Halophila stipulacea (Forsk.) Aschers meadows in the northern Red Sea. *Ecological Indicators*, 60:1150–1163.

Myhre, G., Shindell, D., Bréon, F.-M., Collins, W., Fuglestvedt, J., Huang, J., Koch, D., Lamarque, J.-F., Lee, D., Mendoza, B., Nakajima, T., Robock, A., Stephens, G., Takemura, T., and Zhang, H. (2013). Anthropogenic and Natural Radiative Forcing. In Stocker, T., Qin, D., Plattner, G.-K., Tignor, M., Allen, S. K., Boschung, J., Nauels, A., Xia, Y., Bex, V., and Midgley, P. M., editors, *Climate*

Change 2013: The Physical Science Basis. Contribution of Working Group I to the Fifth Assessment Report of the Intergovernmental Panel on Climate Change, pages 659–740. Cambridge University Press, Cambridge, United Kingdom and New York, NY, USA.

Nurk, S., Bankevich, A., Antipov, D., Gurevich, A., Korobeynikov, A., Lapidus, A., Prjibelsky, A., Pyshkin, A., Sirotkin, A., Sirotkin, Y., Stepanauskas, R., McLean-Roger, J., Lasken, R., Clingenpeel, S. R., Woyke, T., Tesler, G., Alekseyev, M. A., and Pevzner, P. A. (2013). Assembling Genomes and Mini-metagenomes from Highly Chimeric Reads. In: Deng M., Jiang R., Sun F., Zhang X. (eds). In Deng, M., Jiang, R., Sun, F., and Zhang, X., editors, *Research in Computational Molecular Biology. RECOMB 2013. Lecture Notes in Computer Science, vol 7821. Springer, Berlin*, pages 158–170.

Oremland, R. S. (1975). Methane production in shallow-water, tropical marine sediments. *Applied Microbiology*, 30(4):602–608.

Orth, R. J., Carruthers, T. J. B., Dennison, W. C., Duarte, C. M., Fourqurean, J. W., Heck, K. L. J., Hughes, A. R., Kendrick, G. A., Kenworthy, W. J., Olyarnik, S., Short, F. T., Waycott, M., and Williams, S. L. (2006). A global crisis for seagrass ecosystems. *Bioscience*, 56(12):987–996.

Pedersen, M. Ø., Serrano, O., Mateo, M. Á., and Holmer, M. (2011). Temperature effects on decomposition of a Posidonia oceanica mat. *Aquatic Microbial Ecology*, 65:169–182.

Pendleton, L., Donato, D. C., Murray, B. C., Crooks, S., Jenkins, W. A., Sifleet, S., Craft, C., Fourqurean, J. W., Kauffman, J. B., Marbà, N., Megonigal, P., Pidgeon, E., Herr, D., Gordon, D., and Baldera, A. (2012). Estimating Global "Blue Carbon" Emissions from Conversion and Degradation of Vegetated Coastal Ecosystems. *PLoS ONE*, 7(9):e43542.

Piñeiro-Corbeira, C., Barreiro, R., Cremades, J., and Arenas, F. (2018). Seaweed assemblages under a climate change scenario: Functional responses to temperature of eight intertidal seaweeds match recent abundance shifts. *Scientific Reports*, 8(1):1–9.

Por, F. D. (1971). One hundred years of Suez Canal - A century of Lessepsian migration: retrospect and viewpoints. *Systematic Zoology*, 20(2):138–159.

Potts, T. (2018). Climate change, ocean acidification and the marine environment. Challenges for the international legal regime. In Saiful, K. and Daud, H., editors, *International Marine Environmental Law and Policy*. Routledge, London, United Kingdom.

Quast, C., Pruesse, E., Yilmaz, P., Gerken, J., Schweer, T., Yarza, P., Peplies, J., and Glöckner, F. O. (2013). The SILVA ribosomal RNA gene database project: Improved data processing and web-based tools. *Nucleic Acids Research*, 41(D1):590–596.

RCoreTeam (2017). R: A Language and Environment for Statistical Computing, R Foundation for Statistical Computing.

Reeburgh, W. S. (2003). Global Methane Biogeochemistry. In Holland, H. D. and Turekian, K. K., editors, *Treatise On Geochemistry*, pages 1–32. Elsevier.

Robador, A., Brüchert, V., and Jørgensen, B. B. (2009). The impact of temperature change on the activity and community composition of sulfate-reducing bacteria in arctic versus temperate marine sediments. *Environmental Microbiology*, 11(7):1692–1703.

Rogne, T., Flouri, T., Nichols, B., Quince, C., and Mahé, F. (2016). VSEARCH: a versatile open source tool for metagenomics. *PeerJ*, 4:e2584.

Ruiz, H. and Ballantine, D. (2004). Occurrence of the seagrass Halophila stipulacea in the tropical West Atlantic. *Bulletin of Marine Science*, 75:131–135.

Sarmiento, J. L. and Le Quéré, C. (1996). Oceanic carbon dioxide uptake in a model of century-scale global warming. *Science*, 274(5291):1346–1350.

Schlitzer, R. (2016). Ocean Data View, http://odv.awi.de (Accessed on 19 Nov 2018).

Schloss, P. D., Westcott, S. L., Ryabin, T., Hall, J. R., Hartmann, M., Hollister, E. B., Lesniewski, R. A., Oakley, B. B., Parks, D. H., Robinson, C. J., Sahl, J. W., Stres, B., Thallinger, G. G., Van Horn, D. J., and Weber, C. F. (2009). Introducing mothur: Open-source, platform-independent, community-supported software for describing and comparing microbial communities. *Applied and Environmental Microbiology*, 75(23):7537–7541.

Sea, M. A., Garcias-Bonet, N., Saderne, V., and Duarte, C. M. (2018). Carbon dioxide and methane fluxes at the air–sea interface of Red Sea mangroves. *Biogeosciences*, 15(17):5365–5375.

Serrano, O., Almahasheer, H., Duarte, C. M., and Irigoien, X. (2018). Carbon stocks and accumulation rates in Red Sea seagrass meadows. *Scientific Reports*, 8(1):15037.

Shcherbakova, V., Yoshimura, Y., Ryzhmanova, Y., Taguchi, Y., Segawa, T., Oshurkova, V., and Rivkina, E. (2016). Archaeal communities of Arctic methane-containing permafrost. *FEMS Microbiology Ecology*, 92(10):1–11.

Short, F. T. and Neckles, H. A. (1999). The effects of global climate change on seagrasses. *Aquatic Botany*, 63:169–196.

Soetaert, K., Petzoldt, T., Meysman, F., and Meire, L. (2010). marelac: Tools for Aquatic Sciences. R package version 2.1, URL https://cran.r-project.org/package=marelac (Accessed on 19 Nov 2018).

Sotomayor, D., Corredor, J. E., and Morell, J. M. (1994). Methane flux from mangrove sediments along the Southwestern Coast of Puerto Rico. *Coastal and Estuarine Research Federation*, 17(1B):140–147.

Trevathan-Tackett, S. M., Seymour, J. R., Nielsen, D. A., Macreadie, P. I., Jeffries, T. C., Sanderman, J., Baldock, J., Howes, J. M., Steven, A. D., and Ralph, P. J. (2017). Sediment anoxia limits microbial-driven seagrass carbon remineralization under warming conditions. *FEMS Microbiology Ecology*, 93(6):1–15.

Ugarelli, K., Chakrabarti, S., Laas, P., and Stingl, U. (2017). The Seagrass Holobiont and Its Microbiome. *Microorganisms*, 5(81):1–28.

Vandenkoornhuyse, P., Quaiser, A., Duhamel, M., Le Van, A., and Dufresne, A. (2015). The importance of the microbiome of the plant holobiont. *New Phytologist*, 206:1196–1206.

Waycott, M., Duarte, C. M., Carruthers, T. J. B., Orth, R. J., Dennison, W. C., Olyarnik, S., Calladine, A., Fourqurean, J. W., Heck, K. L., Hughes, A. R., Kendrick, G. A., Kenworthy, W. J., Short, F. T., Williams, S. L., and Paine, R. T. (2009). Accelerating loss of seagrasses across the globe threatens coastal ecosystems. *PNAS*, 106(30):12377–12381.

Weidner, S., Arnold, W., Stackebrandt, E., and Pühler, A. (2000). Phylogenetic analysis of bacterial communities associated with leaves of the seagrass Halophila stipulacea by a culture-independent small-subunit rRNA gene approach. *Microbial Ecology*, 39:22–31.

Whiticar, M. J. (1990). A geochemial perspective of natural gas and atmospheric methane. *Organic Geochemistry*, 16(1-3):531–547.

Wiesenburg, D. A. and Guinasso, N. L. J. (1979). Equilibrium Solubilities of Methane, Carbon Monoxide, and Hydrogen in Water and Sea Water. *Journal of Chemical and Engineering Data*, 24(4):356–360.

Wilson, S. T., Böttjer, D., Church, M. J., and Karl, D. M. (2012). Comparative assessment of nitrogen fixation methodologies, conducted in the oligotrophic north pacific ocean. *Applied and Environmental Microbiology*, 78(18):6516–6523.

Zhang, J., Kobert, K., Flouri, T., and Stamatakis, A. (2014). PEAR: a fast and accurate Illumina Paired-End reAd mergeR. *Bioinformatics*, 30:614–620.